REPORT 1230

GENERALIZED INDICIAL FORCES ON DEFORMING RECTANGULAR WINGS IN SUPERSONIC FLIGHT [1]

By Harvard Lomax, Franklyn B. Fuller, and Loma Sluder

SUMMARY

A method is presented for determining the time-dependent flow over a rectangular wing moving with a supersonic forward speed and undergoing small vertical distortions expressible as polynomials involving spanwise and chordwise distances. The solution for the velocity potential is presented in a form analogous to that for steady supersonic flow having the familiar "reflected area" concept discovered by Evvard. Particular attention is paid to indicial-type motions and results are expressed in terms of generalized indicial forces. Numerical results for Mach numbers equal to 1.1 and 1.2 are given for polynomials of the first and fifth degree in the chordwise and spanwise directions, respectively, on a wing having an aspect ratio of 4.

INTRODUCTION

One of the basic problems arising in the analysis of wing flutter boundaries is the calculation of the aerodynamic forces on wings undergoing small but arbitrary spanwise and chordwise distortions. When the wing aspect ratio is large (actually, when the distance between spanwise nodal lines is large), these forces are usually estimated by some strip theory in which the loading on each spanwise section is approximated from that on a two-dimensional wing having the same chordwise distortion. This report is concerned with low-aspect-ratio rectangular wings for which tip effects are important and the full three-dimensional theory must be used.

The exact linearized solution for the forces on thin rectangular wings (limited, however, to the range where effective aspect ratio ($\sqrt{M^2-1}\ A$) is ≥ 1) traveling at supersonic speeds has been presented by both Gardner (ref. 1) and Miles (refs. 2 and 3) in terms of multiple integrals involving arbitrary surface undulations. However, the use of such solutions in evaluating, numerically say, the forces induced by specific wing distortions still presents some difficulties. It is the purpose of this report to discuss certain techniques that can simplify the labor involved in these calculations and to present numerical tables for the forces induced by a class of surface deformations, a class general enough to represent the first few mode shapes of rectangular plates.

Mathematically the problem is to find and analyze a solution to the four-dimensional wave equation

$$\varphi_{xx}+\varphi_{yy}+\varphi_{zz}-\frac{1}{a_0^2}\varphi_{t't't'}=0 \tag{1a}$$

(where a_0 is the speed of sound, t' is the time, and x,y,z are space coordinates) that satisfies the appropriate boundary conditions. The particular form of the solution to be analyzed differs from those presented by Gardner and Miles but its development is based on the method due to Gardner.

Hadamard (ref. 4) studied a generalized form of equation (1a) in which the number of dimensions was arbitrary. His solutions to these generalized equations are fundamentally different, depending on whether the total number of dimensions is odd or even. In fact, the methods Hadamard developed apply directly only to equations for which the total number of dimensions is odd. Solutions for the even cases (such as eq. (1a)) are determined by a "method of descent"; that is, the solution for the next higher odd-dimensioned equation is found and then reduced by (made independent of) one dimension. It is apparent, however, that such a technique is in itself by no means unique. Thus, Hadamard found the solution to equation (1a) by descending from a solution to the equation

$$\varphi_{xx}+\varphi_{yy}+\varphi_{zz}+\varphi_{\xi\xi}-\frac{1}{a_0^2}\varphi_{t't't'}=0 \tag{1b}$$

but there are many other partial differential equations and groups of partial differential equations governing a five-dimensional (x,y,z,ξ,t) space all of which satisfy equation (1a) in a plane $\xi=$constant. Gardner discovered a set of equations containing equation (1a) in a $\xi=$constant plane which are simpler than equation (1a) in that solutions could be found and adapted to the boundary conditions for time-dependent motion by methods well known to aerodynamicists who have studied the flow about wings in steady supersonic flight. This is the essential part of Gardner's contribution and it represents the technique upon which the development of the solution presented in this report is based. Actually, Gardner first applied a Lorentz transformation to equation (1a) and then used his method outlined above. The application of such a transformation is unnecessary and has the disadvantage that the resulting coordinates have lost their direct physical significance. We will apply Gardner's method of descent directly to equation (1a) and then proceed to analyze the solutions so obtained.

In order to simplify the analysis as much as possible, we will limit solutions to the plane of the wing, and, further, consider only indicial-type boundary conditions; in other words, unsteady motions in which the wing attains instantaneously, at the time zero, a certain spanwise and chordwise distortion which is thereafter fixed. It is well known that the transient responses to these indicial motions can be

[1] Supersedes NACA TN 3286 by Harvard Lomax, Franklyn B. Fuller, and Loma Sluder, 1951.

used, in a superposition integral, to obtain responses to many other types of unsteady motion; in particular, responses to the harmonic oscillations of nonrigid wings.

Finally, the principal interpretation of the results will be made in terms of generalized forces, since these can be used directly in either flutter or gust studies, and it will be shown that the amount of labor required to calculate such forces is reduced by using reciprocity relations derived from the general theorems presented in reference 5.

LIST OF IMPORTANT SYMBOLS

A	aspect ratio
a_0	speed of sound
a_{ln}	amplitude of indicial-downwash distribution (See eq. (2a).)
$B(p, q)$	beta function (See eq. (B15a).)
$B_{1-x^2}(p, q)$	incomplete beta function (See eq. (B15b).)
$C(x_1,y_1)$	influence function for effect of side edge (See eq. (A10).)
C_L	lift coefficient, $\frac{\text{lift}}{q_0 S}$
C_{L_α}	indicial lift coefficient due to angle-of-attack change, without pitching, $C_{L_\alpha}=\left.\frac{\partial C_L}{\partial \alpha}\right\|_{\alpha=0}$
C_{L_q}'	indicial lift coefficient due to pitching for a wing rotating about its leading edge, $C_{L_q}=\left.\frac{\partial C_L}{\partial q}\right\|_{q=0}$
C_m	pitching-moment coefficient, positive when trailing edge tends to sink relative to leading edge, $\frac{\text{moment}}{q_0 S c}$
C_{m_α}'	indicial pitching-moment coefficient due to angle-of-attack change (without pitching) measured about the leading edge, $C_{m_\alpha}=\left.\frac{\partial C_m}{\partial \alpha}\right\|_{\alpha=0}$
C_{m_q}'	indicial pitching-moment coefficient due to pitching measured about the leading edge for a wing rotating about its leading edge, $C_{m_q}=\left.\frac{\partial C_m}{\partial q}\right\|_{q=0}$
c	wing chord
$F_{jg}^{ln}(t)$	generalized indicial force coefficient (See eq. (36).)
$f_{jg}^{ln}(t)$	generalized indicial force coefficient (See eq. (37).)
$h(x,y,t)$	distance of wing camber line from $z=0$ plane
M	Mach number
$\frac{\Delta p}{q_0}$	loading coefficient (pressure on the lower surface minus pressure on the upper surface divided by free-stream dynamic pressure)
$\binom{n}{m}$	binominal coefficient, $\binom{n}{m}=\frac{n!}{m!\,(n-m)!}$
q	dimensionless rate of pitching, $\frac{c\dot{\theta}}{U_0}$
q_0	free-stream dynamic pressure, $\frac{1}{2}\rho_0 U_0^2$
q_r	generalized coordinate
Q_r	generalized force corresponding to the generalized coordinate q_r
$R.P.$	real part of
r_0	$\sqrt{(x-x_1)^2+(y-y_1)^2}$
r_1	$\sqrt{(x-x_1)^2+(y+y_1)^2}$
r_c	$\sqrt{(x-x_1)^2-\beta^2(y-y_1)^2}$
s	wing semispan
S	wing area
S_a	area of acoustic plan form
S_c	area of reflected acoustic plan form
t	$a_0 t'$
t'	time
t_0	$\frac{t}{c}$
t_m	$\frac{x+Mt}{\beta}$
T	wing kinetic energy
U	wing potential energy
U_0	forward speed of wing
W	$\left(\frac{\partial \psi}{\partial z}\right)_{z=0}$
w	vertical velocity
x,y,z	Cartesian coordinates, fixed relative to the fluid at infinity
x_3,y_3,t_3	coordinates with origin on center of wing leading edge (See fig. 13.)
x_4,y_4,t_4	coordinates with origin on center of wing leading edge at time zero (See fig. 14.)
x_0	$\frac{x}{c}$
x_m	$\frac{Mx+t}{\beta}$
$X_1(\eta)$	$\frac{M}{\beta}\left(x_m-\sqrt{t_m^2-\eta^2}\right)$
α	angle of attack (angle between flight path and plane of wing), radians
β	$\sqrt{M^2-1}$
θ	wing angle of pitch relative to horizontal, positive when trailing edge lies below leading edge, radians
ξ	coordinate measuring fifth dimension
ρ_o	free-stream density
φ	velocity potential
$\varphi^{(1)}$	portion of velocity potential induced by sources in acoustic plan form
$\varphi^{(2)}$	portion of velocity potential induced by presence of side edge
ψ	potential function in five-dimensional space

Subscripts

A,B,C	regions in an x, ξ plane (See fig. 7.)
u	upper side of wing, $z=0+$
1	singularity (e. g., source) position
$I,II,...,VIII$	regions on wing shown in figure 4

STATEMENT OF THE PROBLEM

THE GOVERNING EQUATION

Assuming a wing's vertical motion is of such a nature that the velocities induced in the fluid are small relative to the magnitude of the wing's steady forward motion, the normalized form of equation (1a)

$$\varphi_{xx}+\varphi_{yy}+\varphi_{zz}-\varphi_{tt}=0 \tag{1c}$$

where $t=a_0t'$, can be used as the governing partial differential equation of the flow field. This equation applies to the determination of the velocity potential when the body or wing in question moves through the fluid, the axes remaining fixed with respect to the still fluid infinitely distant from the origin. For convenience we place the wing leading edge on the y axis at $t=0$ and the side edge on the x axis. The wing flies at a constant forward (in the negative x direction) speed so at subsequent times the leading edge lies along the line $x=-Mt$, where M is the Mach number, and the side edge moves along the x axis as shown in figure 1.

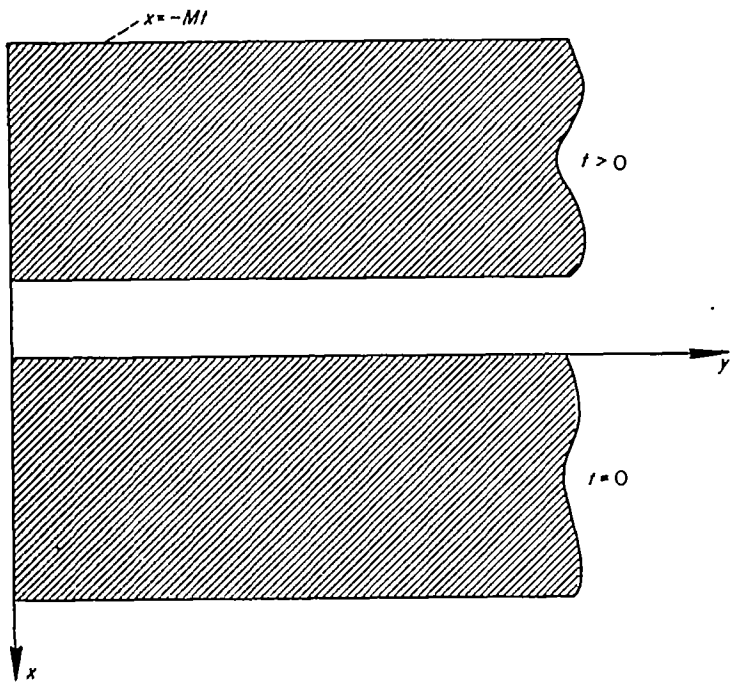

FIGURE 1.—Wing in fixed coordinate system.

THE BOUNDARY CONDITIONS

The fluid velocity normal to the surface of a solid moving in a frictionless fluid must be zero. If the equation of the solid's surface is represented by

$$G(x,y,z,t')=0$$

this boundary condition can be expressed mathematically, in terms of the coordinate system used in equation (1c), as

$$\frac{\partial G}{\partial t'}+\frac{\partial \varphi}{\partial x}\frac{\partial G}{\partial x}+\frac{\partial \varphi}{\partial y}\frac{\partial G}{\partial y}+\frac{\partial \varphi}{\partial z}\frac{\partial G}{\partial z}=0$$

Consider a thin surface near the $z=0$ plane. The equation of the camber line of this surface can then be expressed in the form

$$G(x,y,z,t')=z-h(x,y,t')=0$$

and, assuming that thickness and lifting effects can be separated linearly, the boundary condition for the camber line becomes

$$\frac{\partial h}{\partial t'}+\frac{\partial \varphi}{\partial x}\frac{\partial h}{\partial x}+\frac{\partial \varphi}{\partial y}\frac{\partial h}{\partial y}-\frac{\partial \varphi}{\partial z}=0$$

If the derivatives of h with respect to each of the coordinates are small, the two middle terms can be neglected and the expression for the boundary condition reduces to

$$\frac{\partial h}{\partial t'}\approx\left.\frac{\partial \varphi}{\partial z}\right|_{z=0}=w_u(x,y,t')$$

We wish to simulate a rectangular wing deformed indicially by bending in the spanwise and chordwise directions. For this purpose, on the portion of the $z=0$ plane occupied by the wing plan form, the vertical velocity, which determines the wing shape according to the previous equation, is assumed to have the form

$$w_u=\begin{cases}0 & t<0\\ \sum_l\sum_n a_{ln}\left(\frac{x+Mt}{c}\right)^l\left(\frac{y}{c}\right)^n & t>0\end{cases}$$

where c is chord length, a_{ln} is a constant and l and n are integers ≥ 0.

The expression $(x+Mt)^l$ is used so that for $l>0$ the tangent to the wing camber line at the leading edge is tangent to the flight-path angle of the leading edge. Consider, for example, the case $l=1$, $n=0$. The downwash

$$w_u=\frac{a_{10}}{c}(x+Mt)$$

represents an infinite class of surface shapes having the form

$$h(x,y,t)=\frac{a_{10}}{2cU_0}[(x+Mt)^2+f(x,y)] \qquad (2)$$

where $f(x,y)$ is an arbitrary function and h is, by definition, the distance of the wing's camber line from the $z=0$ plane. Since, within the accuracy of linearized theory, the solution for the flow about the wing depends only upon the value of $w_u(x,y,t)$, the loading on all the wings represented by the above equation is the same.

Let us inspect the two special cases

(i) $f(x,y)=-x^2$

(ii) $f(x,y)=0$

For case (i)

$$h(x,y,t)=\frac{a_{10}M}{2cU_0}(2xt+Mt^2)$$

and the wing is a flat plate pitching at a uniform rate about its leading edge which is following the flight path

$$(h)_{LE}=-\frac{a_{10}M^2t^2}{2cU_0}$$

as shown [2] in figure 2. Hence, at time t the tangent to the flight path of the leading edge is

$$\frac{d(h)_{LE}/dt'}{-U_0}=\frac{a_{10}t'}{c}$$

The slope of the leading edge of the plate at the same time is

$$\left(\frac{\partial h}{\partial x}\right)_{LE}=\frac{a_{10}t'}{c}$$

and the two slopes are seen to be equivalent.

[2] The z scale in both figures 2 and 3 is purposely distorted in order to make the drawings clear. A basic assumption used in setting up the boundary-value problem, by means of which the loading was determined, was that the surface of the wing must remain near the $z=0$ plane.

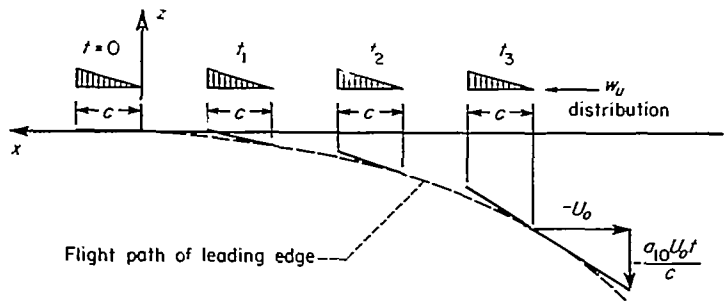

FIGURE 2.—Flat plate pitching at uniform rate about leading edge.

For case (ii)

$$h(x,y,t)=\frac{a_{10}}{2cU_0}(x+Mt)^2$$

and the wing is a plate which obtained a sudden parabolic camber at $t=0$, a shape it maintained thereafter as shown [2] in figure 3.

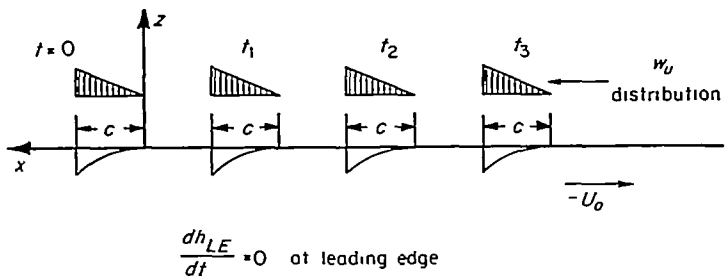

FIGURE 3.—Plate with parabolic camber.

The problem is linear, so it will be sufficient to determine a solution for arbitrary l and n, and then add results for any combination of terms as desired. Thus, the complete boundary conditions to be studied are

$$w_u(x,y,t)=\left.\frac{\partial\varphi}{\partial z}\right|_{z=0}=a_{ln}\left(\frac{x+Mt}{c}\right)^l\left(\frac{y}{c}\right)^n \qquad (2a)$$

over the wing plan form, and, since the loading is zero over the remaining portion of the plane

$$\left.\frac{\partial\varphi}{\partial t}\right|_{z=0}=0 \qquad \text{off the wing} \qquad (2b)$$

since the loading is given by

$$\frac{\Delta p}{q_0}=\frac{4}{U_0M}\left(\frac{\partial\varphi}{\partial t}\right)_{z=0+}$$

SOLUTION FOR THE POTENTIAL

Figure 4 shows the wing plan form on the surface of which the potential is required, together with the system of axes; also, traces in the $z=0$ plane of the wave system set up by the indicial motion of the wing are indicated. The wave pattern for only two edges is shown; the flight speed is supersonic so the trailing edge has no effect on the velocities induced over the wing surface, and the results are valid (in their entirety) only for $\beta A\geq 1$, so the opposite edge either has no effect or one that can be incorporated by simple superposition.

The wave traces divide the wing area into several regions, indicated by the Roman numerals, in each of which the analytical formulation for the potential is different. Region *I* consists of that part of the wing where the effect of neither the side edge nor leading edge has yet been felt. In region *II*, the side-edge influence is acting (the line $y=t$ is the trace of the starting cylindrical wave from the side edge $y=0$) but not the leading edge. Region *III* is the part within the starting cylindrical wave from the leading edge, but outside the influence of the side edge. This region, and region *V*, are further subdivided for reasons that will appear later. Region *IV* is a compound region; potential there can be found by adding the potentials for regions *II* and *III* and subtracting the potential for region *I*. Region *V* consists of the portion of the wing within the spherical wave originating at the wing corner. The flow over the part of the wing comprising regions *VI* and *VII* has reached a steady state relative to a point on the wing, and the potential there is just that for the corresponding parts of a rectangular wing with the proper downwash distribution in steady motion. Finally, region *VIII* is again a composite region, its potential being the sum of potentials for regions *III* and *VII* less the potential for region *VI*.

All the regions just listed, with the exception of region *V*, are actually governed by the three- (total) dimensional wave equation and the potential therein could be obtained by methods applicable to this simpler equation. However, in this report we shall present a unified approach and the problem will be solved by the same method in all regions.

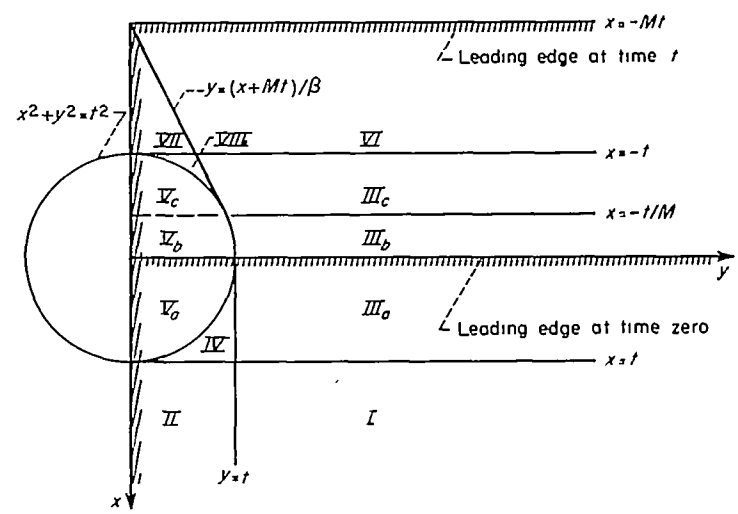

FIGURE 4.—Regions used in the analysis of a rectangular wing in supersonic unsteady motion.

REVIEW OF KIRCHHOFF'S FORMULA

The solutions developed in the subsequent sections are more clearly interpretable if they are compared with certain known results that have already been determined for the indicial motion of nonlifting wings with symmetrical thickness distributions or lifting surfaces with all supersonic edges. The purpose of this section is simply to review briefly some of these latter results.

As in steady-state wing theory, there is a formula for time-dependent flows that relates the velocity potential to a distribution of time-dependent sources and doublets over a certain region in the wing plane. This formula is due to Kirchhoff, and some of its aerodynamic uses are discussed in reference 6. Kirchhoff's result is immediately applicable in the study of unsteady lifting-surface problems when the potential can be represented by sources alone, that is, when the upper and lower surfaces of the wing do not interact, as is the case in regions *I*, *III*, and *VI* of figure 4.

Kirchhoff's formula for source distributions can be written

$$\varphi(x,y,0,t)=-\frac{1}{2\pi}\iint_{S_a}\frac{[w_u]}{r_0}\,dx_1dy_1 \tag{3}$$

where

$$r_o^2=(x-x_1)^2+(y-y_1)^2$$

The brackets on w_u indicate that the retarded value is to be taken

$$[w_u]=w_u(x_1,y_1,t-r_o)$$

and S_a indicates that the region of integration is the acoustic plan form corresponding to the event $(x,y,0,t)$. These concepts are discussed at length in reference 6.

As has been pointed out, equation (3) holds for each of the regions *I*, *III*, and *VI*, but the area of integration S_a differs considerably from one of these regions to another. Consider, for example, the determination of φ for region *III*, denoted φ_{III}. Part of the boundary of the acoustic plan form S_a is found by eliminating T between the equation of the leading edge, $x_1=-MT$, and the expression

$$(x-x_1)^2+(y-y_1)^2=(t-T)^2$$

which gives the outer boundary, at "time" t, of all the disturbances that, operating at "time" T, can produce an effect at the point (x,y). This boundary is the ellipse

$$\left(\frac{\beta}{M}x_1-x_m\right)^2+(y-y_1)^2=t_m^2 \tag{4a}$$

where

$$x_m=\frac{Mx+t}{\beta},\ t_m=\frac{x+Mt}{\beta}$$

If the point (x,y) lies within the cylindrical wave from the leading edge, that is, $-t<x<t$, the ellipse of equation (4a) comprises only part of the acoustic plan form, the remainder being bounded by so much of the circle

$$(x-x_1)^2+(y-y_1)^2=t^2 \tag{4b}$$

as lies on the wing at time zero. Figure 5 shows the three possible acoustic plan forms for points in region *III*. The limits for the three types are

(i) $t\geq x\geq 0$

(ii) $0\geq x\geq -t/M$

(iii) $-t/M\geq x\geq -t$

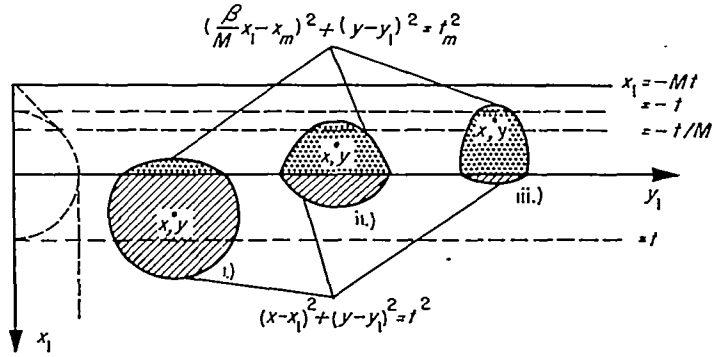

FIGURE 5.—Acoustic plan forms for region *III* of figure 4.

and these correspond to the subregions III_a, III_b, and III_c identified in figure 4. Using equation (3), we can write the potential in, say, region III_a as

$$\varphi_{III_a}=-\frac{1}{2\pi}\int_{y-t}^{y+t}dy_1\int_{x-\sqrt{t^2-(y-y_1)^2}}^{x+\sqrt{t^2-(y-y_1)^2}}\frac{[w_u]}{r_0}\,dx_1+$$

$$\frac{1}{2\pi}\int_{y-\sqrt{t^2-x^2}}^{y+\sqrt{t^2-x^2}}dy_1\int_{x-\sqrt{t^2-(y-y_1)^2}}^{X_1(y-y_1)}\frac{[w_u]}{r_0}\,dx_1 \tag{5}$$

where

$$X_1(y-y_1)=\frac{M}{\beta}\left[x_m-\sqrt{t_m^2-(y-y_1)^2}\right]$$

GARDNER'S METHOD OF DESCENT

Equation (1c) governs a four-dimensional x,y,z,t space. Our object, of course, is to find for this equation a solution that satisfies the boundary conditions in the $z=0$ plane as specified in equations (2a) and (2b). Obviously, we can always construct a space of more dimensions governed in an arbitrary way except that it must satisfy equation (1c) in an x,y,z,t hyperplane. Then, if a solution in this higher dimensional space which satisfies equations (2a) and (2b) in the x,y,z,t plane can be found, it represents for ξ (the additional dimension) equal to some constant the solution to our problem. This characterizes the method of descent. It is not obvious, of course, that such a method leads to any simplification; but, with a proper choice of the governing equation for the new space, such a possibility always exists.

There are examples where various applications of this method have proved to be useful. Hadamard's use of the method, mentioned in the introduction, is classical. A simple application of his method is the derivation of the velocity potential for a source in a two-dimensional supersonic flow field. This potential field (which amounts to a step function, the step occurring at the Mach wave) is easy to derive if one considers a three-dimensional field with a line of sources normal to the free stream and uniform in strength. The two-dimensional field mentioned above follows immediately by descent.

In other examples the additional dimension is measured with imaginary numbers and the additional law for the extended space is the requirement that the functional dependence on the resulting complex variable shall be analytic. The method of descending in the latter case is associated with the study of analytic continuation. In particular, Riesz's method (discussed in ref. 7) for solving equation (1c) illustrates these concepts.

413672—57——39

Gardner's method for solving equation (1c) is to define a five-dimensional space in which a potential function ψ is governed by the equations

$$\psi_{tt}-\psi_{xx}-\psi_{\xi\xi}=0 \tag{6a}$$

$$\psi_{\xi\xi}-\psi_{yy}-\psi_{zz}=0 \tag{6b}$$

and show that solutions to equations (6) in this space are general enough to contain general solutions to equation (1c) in a plane ξ=constant. We shall, therefore, proceed by analyzing these equations and eventually let ξ approach a plane in which the boundary conditions of equations (2a) and (2b) are satisfied. For convenience, the latter plane is taken to be the $\xi=0$ plane.

Since equations (6a) and (6b) are linear, a number of possibilities exist for the choice of the dependent variable $\psi(x, y, z, 0, t)$. Aside from the more obvious choice $\psi(x, y, z, 0, t)=\varphi(x, y, z, t)$, where φ is the velocity potential of equation (1c); for example, one could let $\psi(x, y, z, 0, t)=\varphi_z(x, y, z, t)$ or again, $\psi_\xi(x, y, z, 0, t)=\varphi(x, y, z, t)$. These various choices amount only to relatively minor differences in the detailed technique of the subsequent analysis. If, in imposing the boundary conditions of equations (2), one is to use only source-type solutions for both equations (6a) and (6b), the last choice is sufficient. Therefore, set

$$\left[\frac{\partial}{\partial\xi}\psi(x,y,z,\xi,t)\right]_{\xi=0}=\varphi(x,y,z,t) \tag{7}$$

Now differentiate equation (6a) with respect to z and set [3] $z=0$.

Defining

$$W(\xi,x,y,t)=\left.\frac{\partial\psi}{\partial z}\right|_{z=0} \tag{8}$$

equation (6a) can be expressed in the form

$$W_{tt}-W_{xx}-W_{\xi\xi}=0 \tag{9}$$

and the boundary conditions for equation (9) are given directly by equations (2). Thus on the wing

$$\left.\frac{\partial W}{\partial\xi}\right|_{\xi=0}=\left.\frac{\partial\varphi}{\partial z}\right|_{z=0}=w_u(x,y,t)=a_{lm}\left(\frac{x+Mt}{c}\right)^l\left(\frac{y}{c}\right)^m \tag{10a}$$

and off the wing

$$\left.\frac{\partial W}{\partial t}\right|_{\xi=0}=\varphi_t(x,y,0,t)=0 \tag{10b}$$

Assuming equation (9) to have been solved for the boundary conditions given by equations (10), we return to the second of the set of partial differential equations (6), specifically,

$$\psi_{\xi\xi}-\psi_{yy}-\psi_{zz}=0$$

From equation (8), it is seen that the solution to equation (9) yields the result

$$\left.\frac{\partial\psi}{\partial z}\right|_{z=0}=\text{known function of } y, \xi \text{ on the wing}$$

Further, the boundary conditions for the original problem in (x, y, z, ξ, t) space require that φ be an odd function with respect to z, and continuous across the $z=0$ plane except over the wing plan form. Thus φ must be zero for $z=0$ except over the wing plan form. The continuation of this condition into (x, y, z, ξ, t) space then implies, according to equation (7), that off the wing

$$\left.\frac{\partial\psi}{\partial\xi}\right|_{z=0}=0$$

Hence, both the second partial differential equation and its boundary conditions are identical in form to the first set given by equations (9) and (10), respectively. Applying equation (7) to their dual solution, we obtain the desired result

$$\left[\frac{\partial}{\partial\xi}\psi(x,y,0,\xi,t)\right]_{\xi=0}=\varphi(x,y,0,t)$$

for the potential on a rectangular wing (with $\beta A\geq 1$) in supersonic unsteady motion.

THE GENERAL EXPRESSION FOR THE POTENTIAL

The method outlined in the preceding section will now be applied to obtain integral expressions for the potential in any region of the rectangular wing shown in figure 4. Consider first equation (9) for $W(\xi, x, t)$. This equation is the same partial differential equation as that which governs supersonic steady flow. Further, the boundary values in the ξ, x, t space are identical to those representing a thin planar wing in a steady supersonic flow. Since the Mach number in the steady-flow analog is $\sqrt{2}$, the equivalent plan form of this wing (shown in fig. 6) is a sweptforward wing tip *having all supersonic edges* (i. e., the component of the free-stream velocity normal to all edges is supersonic).

Since all edges of the equivalent wing plan form are supersonic, the solution for W can be written immediately

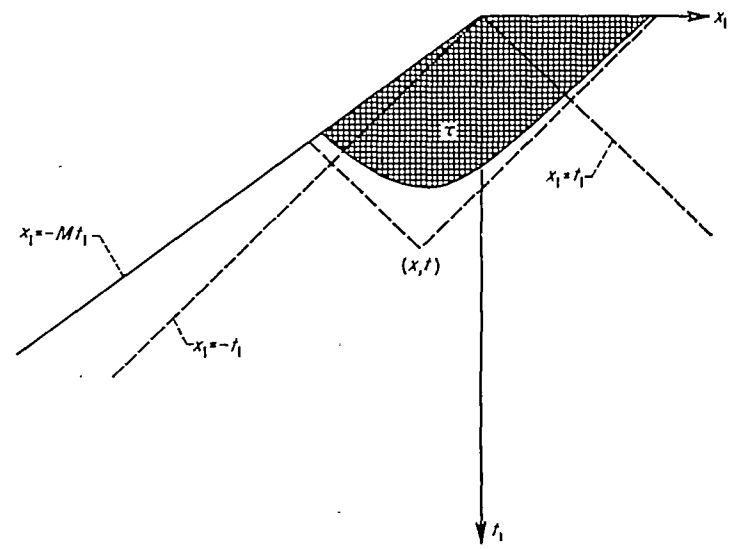

FIGURE 6.—Equivalent plan form in ξ,x,t space.

[3] It can be shown that the solution satisfies the equation

$$\lim_{x\to 0}\left\{\lim_{\xi\to 0}\left[\psi_\xi(x,y,z,\xi,t)\right]\right\}\equiv\lim_{x\to 0}\varphi(x,y,z,t)\equiv\lim_{\xi\to 0}\left\{\lim_{x\to 0}\left[\psi_\xi(x,y,z,\xi,t)\right]\right\}$$

in terms of "sources" only, their strength being given by equation (10a). Thus, by analogy with the well-known results of supersonic wing theory, we have

$$W(\xi,x,t)=-\frac{1}{\pi}\iint_{\tau}\frac{w_u(x_1+Mt_1,y)\,dx_1dt_1}{\sqrt{(t-t_1)^2-\xi^2-(x-x_1)^2}} \tag{11}$$

where τ is the area on the wing cut out by the forecone from the point (ξ, x, t). The analytic form of W will differ considerably in each of the three regions above the equivalent wing shown in figure 7.

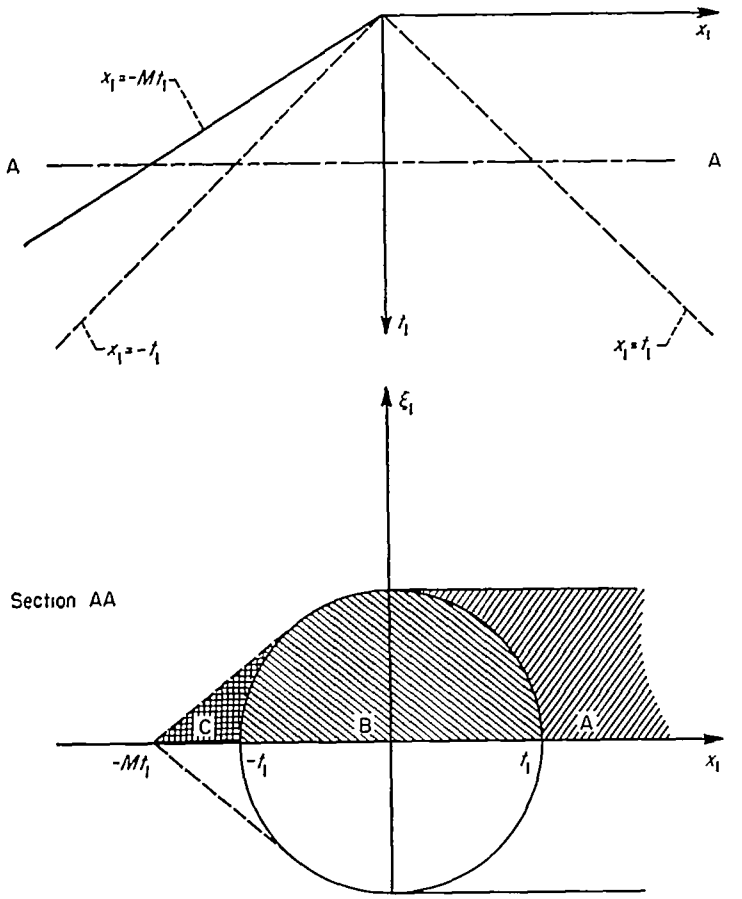

FIGURE 7.—Regions in which analytic form of $W(\xi,x,t)$ differs.

The value of W given by equation (11) now becomes a boundary condition for the solution of equation (6b). Thus, over the portion of the $z=0$ plane for which $y\geq 0$, $\xi\geq 0$, the variation of $\left.\frac{\partial\psi}{\partial z}\right|_{z=0}$ is now known and for $y<0$, $\xi\geq 0$ the condition $\left.\frac{\partial\psi}{\partial\xi}\right|_{z=0}=0$ applies. (These conditions are still not sufficient to determine a unique solution unless the further restriction is imposed that the loading falls to zero as the edge $y=0$ is approached, i. e., as $y\to 0+$.) Again we observe that these boundary conditions and the partial differential equation (6b) are identical to those studied in connection with a stationary planar wing in a supersonic stream. As shown in figure 7, solutions from the t, x, ξ space above the $\xi=0$ plane are referred to as W_A, W_B, and W_C, depending on the relation between x and ξ in a t=constant plane. Figure 8 shows the five different boundary-value problems formed by the various combinations of W_A, W_B, and W_C occurring along constant x lines in the x, ξ plane and the corresponding regions in figure 4 for which each applies. Each of these five problems is directly analogous to the boundary-value problem encountered in steady-state lifting-surface theory, of a planar, rectangular lifting surface in a steady supersonic stream. The "leading edges" of these analogous rectangular plan forms lie along the lines $\xi_1=t$, $\xi_1=\sqrt{t^2-x^2}$ or $\xi_1=t_m$, depending on the value of x,

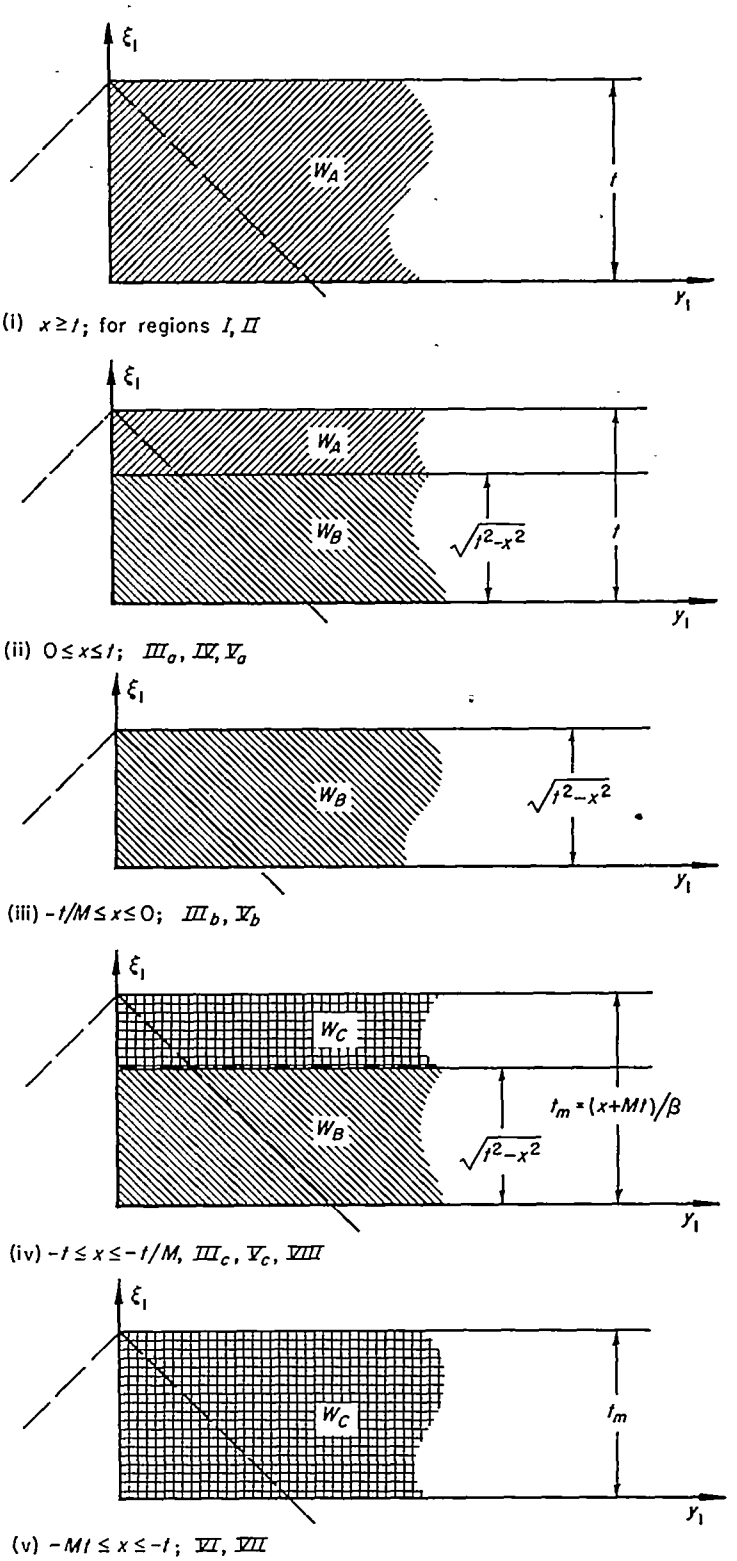

FIGURE 8.—The five different boundary-value problems in ξ_1, y_1, z_1 space.

and the "side edge" lies along the line $y=0$. Hence, by means of this steady-flow analog, we can immediately write the solution to equation (6b) in the form

$$\psi(x,y,0,\xi,t)=-\frac{1}{\pi}\iint_{\sigma}\frac{W(x,y_1,\xi_1,t)\,d\xi_1\,dy_1}{\sqrt{(\xi-\xi_1)^2-(y-y_1)^2}} \tag{12}$$

where only the area of integration σ must be discussed.

Two possibilities exist for the shape of σ. First, if the point ξ, y lies to the right of the dashed lines in figure 8, which in the analogous steady-flow problem represent the traces of the Mach cones from the leading-edge tips, σ is the triangular area shown (for region III_a) in figure 9, part (i). If however, ξ, y lies between this line and the side edge, $y=0$, σ is the trapezoidal area shown (for region V_a) in figure 9, part (ii). The latter is a well-known result used in steady supersonic lifting-surface theory and first developed by Evvard (ref. 8). The division of the five kinds of problems illustrated in figure 8 into the final twelve, represented by the regions in figure 4, is brought about by the various combinations of W_A, W_B, and W_C that can occur in the area σ as the point ξ, y assumes all necessary values on the wing.

When ψ has been determined, the potential in the physical plane is found by equation (7), or, combining equations (11) and (12),

$$\varphi(x,y,0,t)=\frac{1}{\pi^2}\lim_{\xi\to 0}\frac{\partial}{\partial\xi}\iint_{\sigma}\frac{d\xi_1\,dy_1}{\sqrt{(\xi-\xi_1)^2-(y-y_1)^2}}\iint_{\tau}\frac{w_u(x_1+Mt_1,y_1)\,dx_1\,dt_1}{\sqrt{(t-t_1)^2-\xi_1^2-(x-x_1)^2}} \tag{13}$$

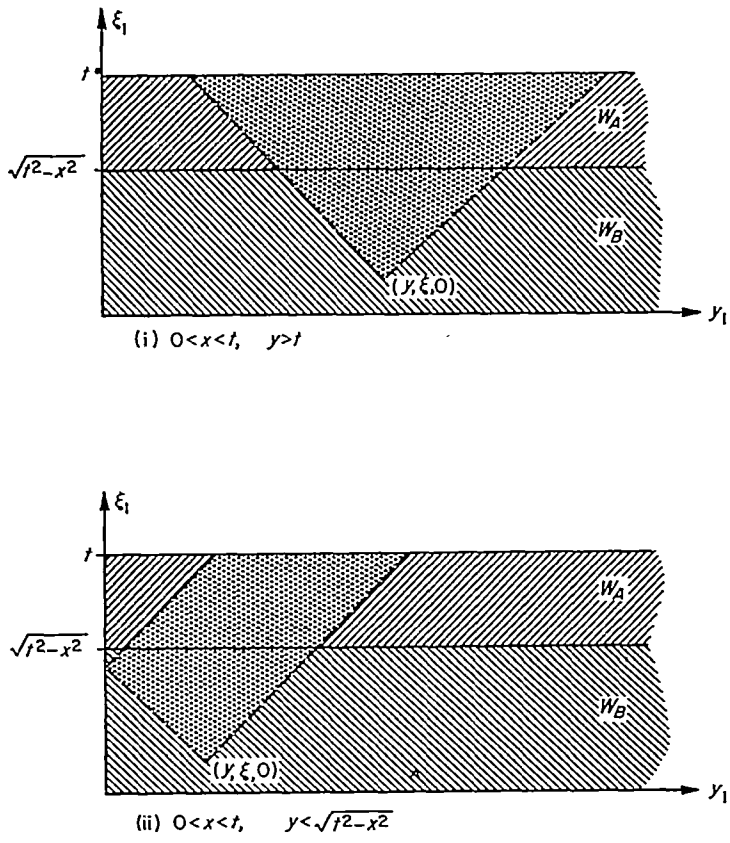

FIGURE 9.—Area of integration σ used in equation (12).

A detailed analysis of equation (13) for a point x, y, t in region V_a of figure 4 is given in Appendix A, and a study of this analysis enables one to write the results for all regions without difficulty.

INTERPRETATION OF THE RESULTS

The results of the rather involved analysis given in Appendix A can be interpreted in terms of the known solutions for simpler boundary conditions. These latter solutions have already been reviewed in a previous section in which it was shown that the potential on a lifting surface with all supersonic edges can be written in the form

$$\varphi(x,y,0,t)=-\frac{1}{2\pi}\iint_{S_a}\frac{[w_u]\,dx_1\,dy_1}{r_0}$$

From Appendix A it is found that the potential at a point on a rectangular lifting surface can always be expressed as the sum of two parts

$$\varphi(x,\,y,\,0,\,t)=\varphi^{(1)}(x,\,y,\,0,\,t)-\varphi^{(2)}(x,\,y,\,0,\,t) \tag{14}$$

where

$$\varphi^{(1)}(x,y,0,t)=-\frac{1}{2\pi}\iint_{S_a}\frac{[w_u]\,dx_1\,dy_1}{r_0} \tag{15a}$$

and

$$\varphi^{(2)}(x,y,\quad,\quad)=-\frac{1}{\pi^2}\iint_{S_c}C(x_1,y_1)\,dx_1\,dy_1 \tag{15b}$$

The value of $C(x_1, y_1)$ is given by equation (A10) in Appendix A and the areas of integration, S_a and S_c, are illustrated for the various regions I through VIII in figure 16.

Let us first inspect equations (15) in light of their possible analogy with the familiar solution for the steady-state, rectangular lifting surface. If a rectangular wing having arbitrary twist and camber is placed in a steady supersonic flow, the solution for the potential on its surface can also be expressed as the sum of two parts

$$\varphi(x,\,y,\,0)=\varphi^{(1)}(x,\,y,\,0)-\varphi^{(2)}(x,\,y,\,0) \tag{16}$$

where, if

$$r_c^2=(x-x_1)^2-\beta^2(y-y_1)^2$$

$$\varphi^{(1)}(x,y,0)=-\frac{1}{\pi}\iint_{S_1}\frac{w_u\,dx_1\,dy_1}{r_c} \tag{17a}$$

and

$$\varphi^{(2)}(x,y,0)=-\frac{1}{\pi}\iint_{S_2}\frac{w_u\,dx_1\,dy_1}{r_c} \tag{17b}$$

These equations can be construed in the following simple way: Equation (17a) represents the potential induced at $x,y,0$ by a distribution of sources over the wing plan form, each source having a strength proportional to the local streamwise slope of the upper surface. The area S_1, as shown in figure 10, is the portion of the wing within the Mach forecone from $x,y,0$. Equation (17b) has a similar interpretation; it also represents a distribution of sources over the wing, each having a strength proportional to the local slope of the upper surface. But the area of integration S_2 is now that portion of the wing within the Mach forecone from the point $x,-y,0$;

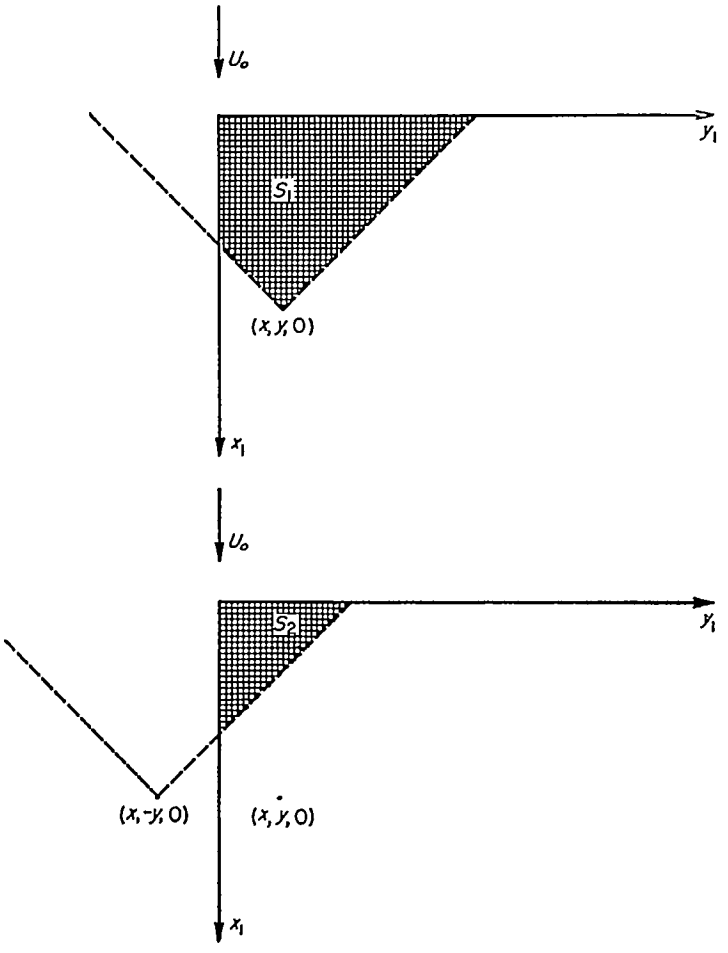

FIGURE 10.—Areas S_1 and S_2 used in equation (17).

that is, within the cone which forms a mirror image of the physical Mach forecone in the vertical plane containing the wing's side edge. The potential $\varphi^{(2)}(x,y,0)$ represents the difference between the potentials for a wing with a vertically symmetrical thickness distribution and a surface with no thickness having the same shape as the upper surface of the nonlifting wing.

Let us return now to equations (15). Just as in the steady-state case, $\varphi^{(1)}(x,y,0,t)$ represents the potential induced at $x,y,0$ by a distribution of sources (see eq. (3)) over the wing plan form, each proportional to the local slope of the wing, but now, since the wing is in motion, with the added condition that they be local slopes at the appropriate time. The area S_a, shown in figure 11, is just the acoustic plan form defined earlier in the discussion of equations (3) and (4). Physically, S_a represents those points on the wing from which disturbances can, at the time t, influence the flow at $x,y,0$. It is the generalization, in the stationary coordinate system, of the wing area bounded by the Mach forecone.

The relation between $\varphi^{(1)}(x,y,0,t)$ and $\varphi^{(2)}(x,y,0,t)$ is similar to that between their steady-state analogs. Thus, again, $\varphi^{(2)}(x,y,0,t)$ represents the difference between the potentials for an uncambered nonlifting wing and a lifting surface having the same shape as the top of the nonlifting wing. A more striking similarity lies in the relation between S_a and S_c.

We have already seen that S_a is the acoustic plan form, and, as it turns out, *S_c is the reflection of the acoustic plan form in the vertical plane containing the side edge* (see fig. 12)—a

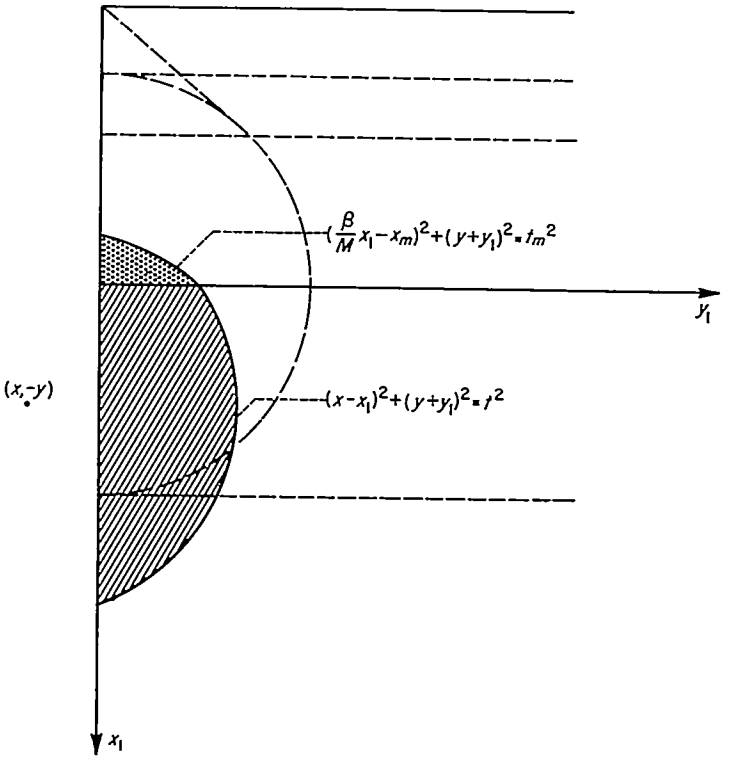

FIGURE 11.—Acoustic plan form for point in region V_a in figure 4.

situation identical to that existing between S_1 and S_2 in the steady-state case. (In other words, S_a is the acoustic plan form for the event $x,y,0,t$, and S_c is the acoustic plan form for the event $x,-y,0,t$.) Physically S_c represents the portion of the wing's lower surface containing disturbances which can, at the time t, influence the flow at $x,y,0$ on the wing's upper surface. At this point the similarity between the steady and unsteady solutions ends since the influence of the slopes in

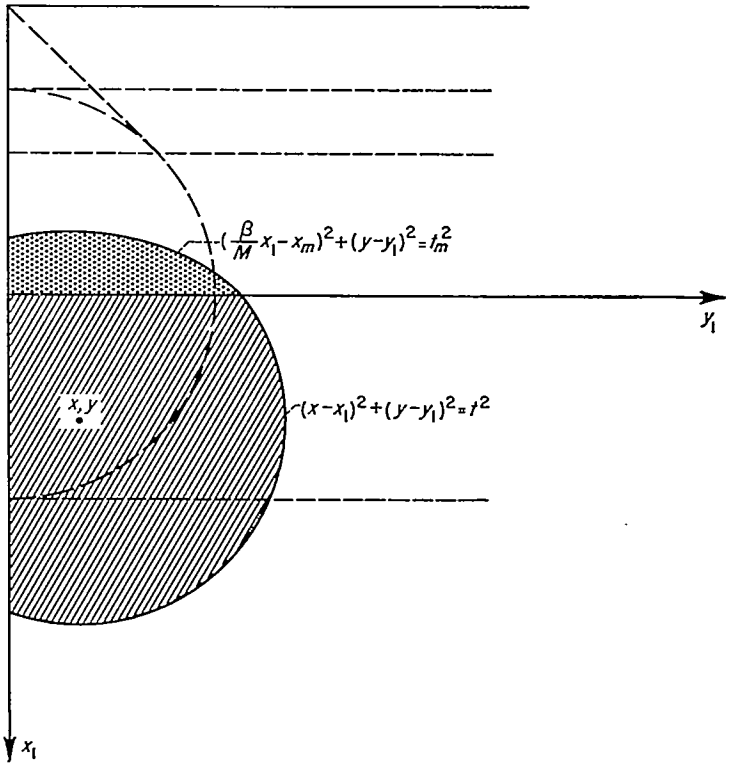

FIGURE 12.—Reflected acoustic plan form for point in region V_a in figure 4.

the reflected plan form is not the same as it is for the slopes in the basic acoustic plan form; the influence in the former case now being given by the integral $C(x_1,y_1)$ defined in equation (A10).

One can show, by simply referring the results given in equations (15) to a coordinate system fixed on the wing, that equations (15a) and (15b) are identical, respectively, to equations (17a) and (17b) when they apply to regions *VII* and *VI* in figure 4; regions in which, for indicial-type motions, the flow is steady relative to the wing. Hence, equations (15a) and (15b) extend Evvard's "reflected area" concept to all parts of a rectangular wing in supersonic unsteady motion.[4]

THE GENERALIZED FORCES

REVIEW OF LAGRANGE'S EQUATIONS OF MOTION

In order to define more clearly the subsequent concepts and notation, we will briefly review Lagrange's equations of motion as applied to distorting wings and will examine a simple application to a rectangular wing.

Lagrange's equations are usually written

$$\frac{d}{dt'}\frac{\partial T}{\partial \dot{q}_r}-\frac{\partial T}{\partial q_r}+\frac{\partial U}{\partial q_r}=Q_r;\ r=1,2,\ \ldots \tag{18}$$

where

T kinetic energy of the wing
U potential energy of wing
Q_r a generalized (external) force
q_r a generalized coordinate

In the present application q_r is the amplitude at a given time of a polynomial measuring h, the vertical displacement of the wing's camber line from the $z=0$ plane. Thus, relative to an x_3,y_3 coordinate system that is fixed on the wing, see figure 13

$$h(x_3,y_3,t')=\sum_s q_s(t')P_s(x_3,y_3) \tag{19}$$

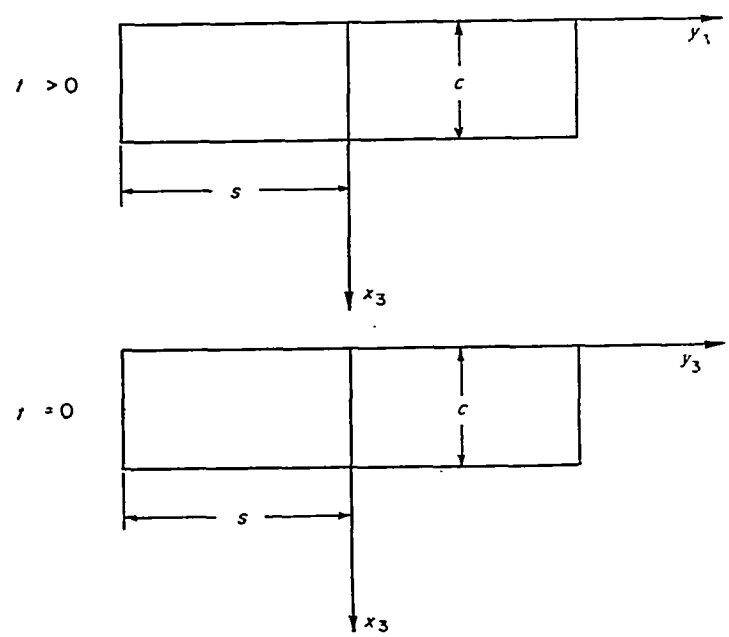

FIGURE 13.—Wing in moving coordinate system.

The wing's kinetic energy can be written

$$T=\iint_S \frac{1}{2}\dot{h}^2 m(x_3,y_3)dx_3dy_3 \tag{20}$$

where m is the wing mass per unit plan form area. Using equation (19), we find

$$\left.\begin{aligned}\frac{d}{dt'}\frac{\partial T}{\partial \dot{q}_r}&=\sum_s \ddot{q}_s\iint_S P_r(x_3,y_3)P_s(x_3,y_3)m(x_3,y_3)dx_3dy_3\\ \frac{\partial T}{\partial q_r}&=0\end{aligned}\right\} \tag{21}$$

The potential energy is usually difficult to evaluate analytically. However, it can often be determined experimentally (as will be seen) by measuring the frequencies of the free vibration modes. For the present assume that the wing is a homogeneous plate of constant thickness. The potential energy for such a wing can be expressed as (ref. 9)

$$U=\frac{D}{2}\iint_S\left\{(\nabla^2 h)^2-2(1-\mu)\left[\frac{\partial^2 h}{\partial y_3^2}\frac{\partial^2 h}{\partial x_3^2}-\left(\frac{\partial^2 h}{\partial x_3\partial y_3}\right)^2\right]\right\}dx_3dy_3 \tag{22}$$

which leads to the equation

$$\frac{\partial U}{\partial q_r}=D\sum_s q_s\iint_S\left[\nabla^2P_r\nabla^2P_s-2(1-\mu)\left(\frac{1}{2}\frac{\partial^2P_r}{\partial y_3^2}\frac{\partial^2P_s}{\partial x_3^2}+\frac{1}{2}\frac{\partial^2P_r}{\partial x_3^2}\frac{\partial^2P_s}{\partial y_3^2}-\frac{\partial^2P_r}{\partial x_3\partial y_3}\frac{\partial^2P_s}{\partial x_3\partial y_3}\right)\right]dx_3dy_3 \tag{23}$$

where μ is Poisson's ratio, $\nabla^2\equiv\partial^2/\partial x_3^2+\partial^2/\partial y_3^2$, and

$$D=\frac{2(\text{Young's modulus})(\text{plate thickness})^3}{3(1-\mu^2)}$$

Now, if the generalized coordinates have been normalized so that each measures the amplitude of a free vibration mode, all terms in equations (21) and (23) involving the integral of the product of P_r and P_s are zero. Assuming, henceforth, such normalization, we can write

$$\ddot{q}_r\iint_S P_r^2(x_3,y_3)m(x_3,y_3)dx_3dy_3+Dq_r\iint_S\left\{(\nabla^2P_r)^2-2(1-\mu)\left[\frac{\partial^2P_r}{\partial x_3^2}\frac{\partial^2P_r}{\partial y_3^2}-\left(\frac{\partial^2P_r}{\partial x_3\partial y_3}\right)^2\right]\right\}dx_3dy_3=Q_r;\qquad r=1,2,\ \ldots \tag{24}$$

Finally, dividing through by the coefficient of $\ddot{q}_r$ and expressing a generalized force as the integral over the wing plan form of the product of the rth mode shape and the loadings [5] $\Sigma(\Delta p)_s$ induced on the wing by each of the mode shapes considered, we find

$$\ddot{q}_r+q_r\omega_r^2=\frac{q_0\sum_s\iint_S P_r(x_3,y_3)\left(\frac{\Delta p}{q_0}\right)_s dx_3dy_3}{\iint_S P_r^2(x_3,y_3)m(x_3,y_3)dx_3dy_3} \tag{25}$$

where ω_r is the frequency of the rth free vibration mode.

[4] It is of further interest to notice that equation (15b) can be reduced to a double integral involving $w_s(\xi,y_1)$ by using, for example, the transformations $\xi=x_1+Mt_1$ and $\tau=t-t_1$ and integrating with respect to τ.

[5] We will write $(\Delta p)_s=q_0(\Delta p/q_0)_s$ where q_0 is the free-stream dynamic pressure. This is possible without a confusion of notation since the generalized coordinates are expressed as $q_1,q_2,q_3,\ \ldots$ and exclude the term q_0.

If the free-mode frequencies are experimentally determined, equations—such as equation (23)—giving the wing's potential energy, never have to be evaluated. Further, in such cases, equation (25) applies to quite general wing structures with varying density. Usually in the application of equation (25), one uses the actual frequency ω_r of the free mode but, in evaluating the aerodynamic forces, uses an analytical expression that only approximates the rth mode shape. Let us examine the generalized force term in equation (25), taking, for simplicity, only one term of the sum:

$$Q_r=q_0\iint_S P_r(x_3,y_3)\left(\frac{\Delta p}{q_0}\right)_s dx_3dy_3 \tag{26}$$

According to what has gone before, the mode shape polynomial $P_r(x_3,y_3)$ has the form

$$P_r(x_3,y_3)=\left(\frac{x_3}{c}\right)^j\left(\frac{y_3}{c}\right)^g \tag{27}$$

while $(\Delta p/q_0)_s$ is the loading coefficient corresponding to an indicial deflection (see previous section on boundary conditions)

$$h=\frac{c}{l+1}q_s(1)\left(\frac{y_3}{c}\right)^n\left[\left(\frac{x_3}{c}\right)^{l+1}+f\left(\frac{y_3}{c},\frac{x_3-Mt}{c}\right)\right] \tag{28}$$

which gives a vertical velocity distribution

$$w_u=U_0q_s(1)\left(\frac{x_3}{c}\right)^l\left(\frac{y_3}{c}\right)^n \tag{29}$$

Now a generalized indicial force coefficient can be defined as follows:

$$f_{jg}^{ln}(t')=\frac{1}{S}q_s(1)\iint_S\left(\frac{x_3}{c}\right)^j\left(\frac{y_3}{c}\right)^g[(\Delta p/q_0)_s]dx_3dy_3 \tag{30}$$

(The calculation of these quantities $f_{jg}^{ln}(t')$ will be elaborated in the next section.) Since the generalized force Q_r is intended to apply to any motion, not necessarily indicial, it is necessary to apply Duhamel's integral to the indicial force coefficient $f_{jg}^{ln}(t')$; thus,

$$Q_r=q_oS\frac{d}{dt'}\int_0^{t'}q_s(t'-\tau')\left[\frac{f_{jg}^{ln}(\tau')}{q_s(1)}\right]d\tau' \tag{31}$$

As an example, consider now a simple one degree of freedom vibrating plate. The plate is fixed to a wall and restrained along its leading edge. The mode shape is assumed to have the form

$$h=cq_1(t')\left(\frac{x_3}{c}\right)^2\left(\frac{y_3}{c}\right)^2 \tag{32}$$

so for a plate with uniform density and thickness

$$m\int_{-s}^{0}dy_3\int_0^c dx_3P_r^2(x_3,y_3)=\frac{msc}{25}\left(\frac{s}{c}\right)^4$$

Equation (25) now becomes

$$\ddot{q}_1+\omega_1^2q_1=\frac{25}{msc}\left(\frac{c}{s}\right)^4Q_1 \tag{33}$$

For this case, we have the generalized indicial force coefficients $f_{22}^{13}(t')$, and $f_{23}^{22}(t')$;

$$Q_1=q_0sc\frac{d}{dt'}\int_0^{t'}\left\{2q_1(t'-\tau')\left[\frac{f_{22}^{13}(\tau')}{q_1(1)}\right]+\frac{c}{U_o}\dot{q}_1(t'-\tau')\left[\frac{f_{23}^{22}(\tau')}{\frac{c}{U_o}\dot{q}_1(1)}\right]\right\}d\tau' \tag{34}$$

Therefore, equation (33) can be written

$$\ddot{q}_1+\omega_1^2q_1=\frac{25q_0}{m}\left(\frac{c}{s}\right)^4\frac{d}{dt'}\int_0^{t'}\left\{2q_1(t'-\tau')\left[\frac{f_{22}^{13}(\tau')}{q_1(1)}\right]+\frac{c}{U_o}\dot{q}_1(t'-\tau')\left[\frac{f_{22}^{22}(\tau')}{\frac{c}{U_o}\dot{q}_1(1)}\right]\right\}d\tau' \tag{35}$$

THE GENERALIZED INDICIAL FORCE COEFFICIENT

It is clear from the previous section that a study of the dynamic behavior of rectangular wings moving at supersonic speeds can be carried out if one can obtain values of the generalized force coefficient, $f_{jg}^{ln}(t')$, as defined by equation (30). We will now show how these values can be obtained from the solution to the aerodynamic boundary-value problem represented by equation (14).

It was convenient in developing equation (14) to use a coordinate system—x,y,z,t—which was fixed in space so that the left edge of the wing moved along the x axis as shown in figure 1. On the other hand, in studying the dynamic problem it was more convenient to use an x_3,y_3,z_3,t system which is fixed on the wing. In order to convert the results in one coordinate set to the other, let us first transfer results in the x,y,z,t set to the x_4,y_4,z_4,t set (shown in figure 14) and then, finally, transfer to x_3,y_3,z_3,t coordinates.

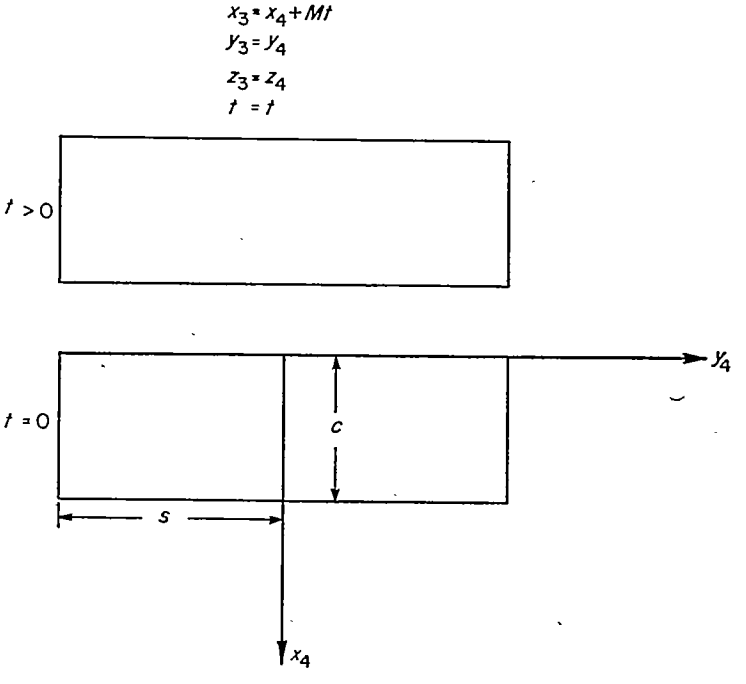

FIGURE 14.—Transformations from moving to fixed coordinate system.

The indicial force coefficient $F_{jg}^{ln}(t')$ is defined as follows:

$$F_{jg}^{ln}(t')=\frac{1}{sc}\int_{-Mt}^{c-Mt}dx\int_0^s dy\left(\frac{x+Mt}{c}\right)^j\left(\frac{y}{c}\right)^g\left(\frac{\Delta p}{q_0}\right)^{ln} \tag{36}$$

In order to transfer the axes from the set shown in figure 1 to the more convenient set of figure 14, so that mode shapes are symmetric or asymmetric about the wing's spanwise center line and the force coefficients denoted f_{jg}^{ln} can be determined, we proceed as follows. First, the loading coefficient for a wing in the (x,y) system with downwash given by

$$\frac{w_u}{U_0}=\left(\frac{x+Mt}{c}\right)^l\left(\frac{y-s}{c}\right)^n$$

$$=\left(\frac{x+Mt}{c}\right)^l(-1)^n\sum_{\mu=0}^{n}(-1)^\mu\binom{n}{\mu}\left(\frac{A}{2}\right)^{n-\mu}\left(\frac{y}{c}\right)^\mu$$

is obtained. This loading coefficient can be written as a sum:

$$\left(\frac{\Delta P}{q_0}\right)^{ln}=(-1)^n\sum_{\mu=0}^{n}(-1)^\mu\binom{n}{\mu}\left(\frac{A}{2}\right)^{n-\mu}\left(\frac{\Delta p}{q_0}\right)^{l\mu}$$

Now the quantity f_{jg}^{ln} is defined in the x_4,y_4,z_4,t system as

$$f_{jg}^{ln}=\frac{1}{2sc}\int_{-Mt}^{c-Mt}dx_4\int_{-s}^{s}dy_4\left(\frac{x_4+Mt}{c}\right)^j\left(\frac{y_4}{c}\right)^g\left(\frac{\Delta P}{q_0}\right)^{ln}$$

$$=\frac{1}{2sc}\int_{-Mt}^{c-Mt}dx\int_0^{2s}dy\left(\frac{x+Mt}{c}\right)^j\left(\frac{y-s}{c}\right)^g\left(\frac{\Delta P}{q_0}\right)^{ln}$$

This last integral can be written as

$$f_{jg}^{ln}=\frac{1}{2sc}[1+(-1)^{g+n}]\int_{-Mt}^{c-Mt}dx\int_0^s dy\left(\frac{x+Mt}{c}\right)^j\left(\frac{y-s}{c}\right)^g\left(\frac{\Delta P}{q_0}\right)^{ln}$$

$$=(-1)^{g+n}\frac{[1+(-1)^{g+n}]}{2}\sum_{\nu=0}^{g}(-1)^\nu\binom{g}{\nu}\left(\frac{A}{2}\right)^{g-\nu}\sum_{\mu=0}^{n}(-1)^\mu\binom{n}{\mu}$$

$$\left(\frac{A}{2}\right)^{n-\mu}\frac{1}{sc}\int_{-Mt}^{c-Mt}dx\int_0^s dy\left(\frac{x+Mt}{c}\right)^j\left(\frac{y}{c}\right)^\nu\left(\frac{\Delta p}{q_0}\right)^{l\mu}$$

By using equation (36) we find

$$f_{jg}^{ln}=\frac{[1+(-1)^{g+n}]}{2}\sum_{\nu=0}^{g}(-1)^\nu\binom{g}{\nu}\left(\frac{A}{2}\right)^{g-\nu}\sum_{\mu=0}^{n}$$

$$(-1)^\mu\binom{n}{\mu}\left(\frac{A}{2}\right)^{n-\mu}F_{j\nu}^{l\mu} \tag{37}$$

where all forces are responses to a unit indicial disturbance. Note that if equation (37) is applied in the case of a wing cantilevered on a wall, both n and g must be even in order to satisfy the boundary conditions of reflection in the wall.

By superimposing boundary conditions and their resulting solutions, one can further show that the value of f_{jg}^{ln} given by equation (37) is valid for all reduced aspect ratios βA greater than 1 in spite of the fact that the value of F_{jg}^{ln} given by equation (36), as it stands, applies only to wings for which βA is greater than 2.

Given $f_{jg}^{ln}(t')$, one can determine the generalized force associated with the generalized coordinate q_r by means of the superposition integral as illustrated by equation (34).

DETAILS OF CALCULATION

The details of actually evaluating the indicial force coefficients from the solution for the potential presented in the first part of this report are discussed in Appendix B. Considerable labor is involved in such calculations, and an attempt was made to discover recursion formulas by means of which certain derivatives, for the rectangular wing, could be expressed as combinations of others. This attempt was successful and yielded the following results:

Consider equation (36). Integrate the x integral in this equation by parts, setting

$$u(x)=\int_0^s y^g\frac{\Delta p^{ln}}{q_0}dy;\qquad dv(x)=(x+Mt)^j dx$$

Then, since by equation (B7) in Appendix B

$$\frac{\partial}{\partial x}\frac{\Delta p^{ln}}{q_0}=\frac{l}{c}\frac{\Delta p^{l-1,n}}{q_0},\ l>0$$

one finds

$$F_{jg}^{ln}=\frac{l}{j+1}\{F_0^{l-1,n}{}_g-F_{j+1,g}^{l-1,n}\} \tag{38a}$$

Inspection of equation (37) shows that the same relation holds for the generalized indicial force coefficients f_{jg}^{ln}; that is,

$$f_{jg}^{ln}=\frac{l}{j+1}\{f_0^{l-1,n}{}_g-f_{j+1,g}^{l-1,n}\} \tag{38b}$$

From this relation, it is seen that only the forces F_{jg}^{0n} need be determined by integration; the forces for higher values of the index l can be found by combination of results for different values of the mode shape index j.

As a simple illustration of the results presented so far, we can calculate the indicial force derivative for the cases $l=n=g=0$, $j=0$, 1. The case $j=0$ corresponds to the indicial lift coefficient for a flat, sinking, rectangular wing, and the case for $j=1$ corresponds to the indicial pitching-moment coefficient for the same wing. Since $n=g=0$, equation (37) gives

$$f_{j0}^{00}=F_{j0}^{00}$$

Thus, with $j=0$ and identifying $-a_{00}/U_0$ as angle of attack α, one finds from Appendix B

$$C_{L_\alpha}=-\frac{1}{a_{00}/U_0}f_{00}^{00}=\frac{4}{M}\left[1-\frac{t_0}{A}\left(1-\frac{Mt_0}{2}\right)\right];\qquad 0\le t_0\le\frac{1}{M+1}$$

$$=\frac{4}{M}\left\{\frac{1}{\pi}\left[\cos^{-1}\frac{Mt_0-1}{t_0}+\frac{M}{\beta}\cos^{-1}(M-\beta^2t_0)+\right.\right.$$

$$\left.\left.\sqrt{t_0^2-(1-Mt_0)^2}\right]-\frac{1}{4A}\left[\frac{1}{M+1}+2t_0-(M-1)t_0^2\right]\right\};$$

$$\frac{1}{M+1}\le t_0\le\frac{1}{M-1}$$

$$=\frac{4}{\beta}\left(1-\frac{1}{2\beta A}\right);\qquad t_0\ge\frac{1}{M-1}$$

Next with $j=1$, and using C_{m_α}' to designate the pitching moment measured about the leading edge of the wing,

$$C_{m_\alpha}'=-\left(-\frac{1}{a_{00}/U_0}\right)f_{10}^{00}=-\frac{2}{M}\left\{\left(1-\frac{1}{2}t_0^2\right)-\frac{t_0}{3A}\left[3-(M^2+1)t_0^2\right]\right\};\quad 0\leq t_0\leq\frac{1}{M+1}$$

$$=-\frac{2}{M}\left\{\frac{1}{\pi}\left[\left(1-\frac{t_0^2}{2}\right)\cos^{-1}\frac{Mt_0-1}{t_0}+\frac{M}{\beta}\cos^{-1}(M-\beta^2t_0)+\frac{1+Mt_0}{2}\sqrt{t_0^2-(1-Mt_0)^2}\right]-\frac{1}{6A}\left[\frac{2}{M+1}+3t_0-(M-1)^2t_0^3\right]\right\};\quad\frac{1}{M+1}\leq t_0\leq\frac{1}{M-1}$$

$$=-\frac{2}{\beta}\left(1-\frac{2}{3\beta A}\right);\quad t_0\geq\frac{1}{M-1}$$

These expressions agree with those given by Miles in reference 2.

The above results can be used to demonstrate the usefulness of equation (38a). Taking $j=n=g=0$, $l=1$ in that equation gives

$$F_{00}^{10}=F_{00}^{00}-F_{10}^{00}$$

or, for the present case,

$$f_{00}^{10}=f_{00}^{00}-f_{10}^{00}$$

which represents the equality

$$C_{L_q}'=C_{L_\alpha}+C_{m_\alpha}'$$

that is, the lift coefficient for a pitching wing equals the sum of the lift and pitching-moment coefficients of a sinking wing (primes indicate the wing is pitching about and moments are measured about the wing leading edge). Hence,

$$C_{L_q}'=\frac{2}{M}\left\{\left(1+\frac{1}{2}t_0^2\right)-\frac{1}{A}\left[t_0-Mt_0^2+\frac{M^2+1}{3}t_0^3\right]\right\};\quad 0\leq t_0\leq\frac{1}{M+1}$$

$$=\frac{2}{M}\left\{\frac{1}{\pi}\left[\left(1+\frac{1}{2}t_0^2\right)\cos^{-1}\frac{Mt_0-1}{t_0}+\frac{M}{\beta}\cos^{-1}(M-\beta^2t_0)+\frac{3-Mt_0}{2}\sqrt{t_0^2-(1-Mt_0)^2}\right]-\frac{1}{6A}\left[\frac{1}{M+1}+3t_0-3(M-1)t_0^2+(M-1)^2t_0^3\right]\right\};\quad\frac{1}{M+1}\leq t_0\leq\frac{1}{M-1}$$

$$=\frac{2}{\beta}\left\{1-\frac{1}{3\beta A}\right\};\quad t_0\geq\frac{1}{M-1}$$

A further application of equation (38a) provides the pitching-moment coefficient for a pitching flat rectangular wing. Thus, with $l=j=1$, $n=g=0$, equation (38a) gives

$$F_{10}^{10}=\tfrac{1}{2}(F_{00}^{00}-F_{20}^{00})$$

which becomes

$$f_{10}^{10}=\tfrac{1}{2}(f_{00}^{00}-f_{20}^{00})$$

and so

$$C_{m_q}'=\frac{1}{2}\left(\frac{f_{20}^{00}}{-a_{00}/U_0}-C_{L_\alpha}\right)$$

From equation (B21) in Appendix B it is found that

$$\frac{f_{20}^{00}}{-\frac{a_{00}}{U_0}}=\frac{F_{20}^{00}}{-\frac{a_{00}}{U_0}}=\frac{4}{M}\left\{\frac{1}{3}(1-Mt_0^3)-\frac{t_0}{12A}\left[4-M(M^2+3)t_0^3\right]\right\};\quad 0\leq t_0\leq\frac{1}{M+1}$$

$$=\frac{4}{M}\left\{\frac{1}{\pi}\left[\frac{1-Mt_0^3}{3}\cos^{-1}\frac{Mt_0-1}{t_0}+\frac{1}{3}\frac{M}{\beta}\cos^{-1}(M-\beta^2t_0)+\frac{1+Mt_0+(M^2+2)t_0^2}{9}\sqrt{t_0^2-(1-Mt_0)^2}\right]-\frac{1}{24A}\left[\frac{3}{M+1}+4t_0-(M-1)^3t_0^4\right]\right\};\quad\frac{1}{M+1}\leq t_0\leq\frac{1}{M-1}$$

$$=\frac{4}{\beta}\left\{\frac{1}{3}-\frac{1}{4\beta A}\right\};\quad t_0\geq\frac{1}{M-1}$$

Combining, we find

$$C_{m_q}'=-\frac{2}{M}\left\{\frac{2+Mt_0^3}{3}-\frac{t_0}{12A}\left[8-6Mt_0+M(M^2+3)t_0^3\right]\right\};\quad 0\leq t_0\leq\frac{1}{M+1}$$

$$=-\frac{2}{M}\left\{\frac{1}{\pi}\left[\frac{2+Mt_0^3}{3}\cos^{-1}\frac{Mt_0-1}{t_0}+\frac{2}{3}\frac{M}{\beta}\cos^{-1}(M-\beta^2t_0)+\frac{8-Mt_0-(M^2+2)t_0^2}{9}\sqrt{t_0^2-(1-Mt_0)^2}\right]-\frac{1}{24A}\left[\frac{3}{M+1}+8t_0-6(M-1)t_0^2+(M-1)^3t_0^4\right]\right\};\quad\frac{1}{M+1}\leq t_0\leq\frac{1}{M-1}$$

$$=-\frac{2}{\beta}\left\{\frac{2}{3}-\frac{1}{4\beta A}\right\};\quad t_0\geq\frac{1}{M-1}$$

Another relation among the generalized indicial forces f_{jg}^{ln} can be derived by means of the reciprocity relations given in reference 5. The details of the derivation are given in Appendix C and there results

$$\sum_{\mu=0}^{j}(-1)^{\mu}\binom{j}{\mu}f_{\mu g}^{ln}=\sum_{\mu=0}^{l}(-1)^{\mu}\binom{l}{\mu}f_{\mu n}^{jg} \tag{39}$$

Equation (39) can be used in two ways; one, as a means for checking the internal consistency of a set of calculated generalized indicial forces, and the other, as a means for expressing a given force in terms of a set of others.

Consider, as an example of the former use, the case for which $l=j=0$. Then

$$f_{0g}^{0n}=f_{0n}^{0g}$$

From equation (37) we can express this relation in terms of the calculated quantities F_{0g}^{0n} thus

$$\sum_{\nu=0}^{n}(-1)^{\nu}\binom{n}{\nu}\sum_{\mu=0}^{g}(-1)^{\mu}\binom{g}{\mu}\left(\frac{A}{2}\right)^{g+n-\mu-\nu}F_{0\nu}^{0\mu}=$$

$$\sum_{\nu=0}^{g}(-1)^{\nu}\binom{g}{\nu}\sum_{\mu=0}^{n}(-1)^{\mu}\binom{n}{\mu}\left(\frac{A}{2}\right)^{g+n-\nu-\mu}F_{0\nu}^{0\mu}$$

If now $n=1$, $g=3$ the following relation results

$$(F_{01}^{03}-F_{03}^{01})+\frac{A}{2}[(F_{03}^{00}-F_{00}^{03})+3(F_{02}^{01}-F_{01}^{02})]+$$

$$3\left(\frac{A}{2}\right)^{2}(F_{00}^{02}-F_{02}^{00})+2\left(\frac{A}{2}\right)^{3}(F_{01}^{00}-F_{00}^{01})=0$$

which provides a useful check on the computed quantities.

Next let us solve equation (39) for a given force. Perform the sum operation

$$\sum_{j=0}^{J}(-1)^{j}\binom{J}{j}$$

on both sides of equation (39), and reverse the order of summation on the left side. There results

$$\sum_{\mu=0}^{J}(-1)^{\mu}f_{\mu g}^{ln}\sum_{j=\mu}^{J}(-1)^{j}\binom{J}{j}\binom{j}{\mu}=\sum_{j=0}^{J}(-1)^{j}\binom{J}{j}\sum_{\mu=0}^{l}(-1)^{\mu}\binom{l}{\mu}f_{\mu n}^{jg} \tag{40}$$

The inner sum on the left can be evaluated. Thus one has

$$x^{p}=[1-(1-x)]^{p}=\sum_{\mu=0}^{p}(-1)^{\mu}\binom{p}{\mu}(1-x)^{\mu}$$

$$=\sum_{\mu=0}^{p}(-1)^{\mu}\binom{p}{\mu}\sum_{r=0}^{\mu}(-1)^{r}\binom{\mu}{r}x^{r}$$

$$=\sum_{r=0}^{p}(-1)^{r}x^{r}\sum_{\mu=r}^{p}(-1)^{\mu}\binom{p}{\mu}\binom{\mu}{r}$$

Equating coefficients of x,

$$\sum_{\mu=r}^{p}(-1)^{\mu}\binom{p}{\mu}\binom{\mu}{r}=\begin{cases}0; & r<p\\ (-1)^{p}; & r=p\end{cases}$$

and equation (40) becomes

$$f_{Jg}^{ln}=\sum_{j=0}^{J}(-1)^{j}\binom{J}{j}\sum_{\mu=0}^{l}(-1)^{\mu}\binom{l}{\mu}f_{\mu n}^{jg}$$

CONCLUDING REMARKS

A method is presented for evaluating the generalized forces on a rectangular wing flying at supersonic speeds and having an aspect ratio such that $\beta A\geq 1$. The generalized coordinates used to define the wing's behavior are the amplitudes of downwash distributions expressed in terms of polynomials in x and y, the chordwise and spanwise directions, respectively.

Numerical results are presented in table I for generalized indicial forces on a wing having an aspect ratio of 4 and flying at a Mach number equal to 1.1 and 1.2; the polynomial coverage being $0\leq l\leq 1$ and $0\leq n\leq 5$, where $w\sim x^{l}y^{n}$.

AMES AERONAUTICAL LABORATORY
NATIONAL ADVISORY COMMITTEE FOR AERONAUTICS
MOFFETT FIELD, CALIF., *June 30, 1954*

APPENDIX A

EXPRESSIONS FOR THE POTENTIAL

In order to write the expressions for the potential in all regions shown in figure 4, it is sufficient to derive in detail only that for region V. Having carried out this analysis, one can determine the expressions for potential in other regions without difficulty.

Consider, therefore, equation (13) and let σ and τ apply to region V_a. First, it is necessary to determine the potentials W_A and W_B in the t,x,ξ space. From equation (11), in conjunction with figure 7, it is found that

$$W_A=-\frac{1}{\pi}\int_{x-\sqrt{t^2-\xi_1^2}}^{x+\sqrt{t^2-\xi_1^2}} dx_1 \int_0^{t-\sqrt{(x-x_1)^2+\xi_1^2}} \frac{w_u(x_1+Mt_1,y_1)dt_1}{\sqrt{(t-t_1)^2-\xi_1^2-(x-x_1)^2}} \tag{A1}$$

$$W_B=-\frac{1}{\pi}\int_{X_1(\xi_1)}^{0} dx_1 \int_{-x_1/M}^{t-\sqrt{(x-x_1)^2+\xi_1^2}} \frac{w_u(x_1+Mt_1,y_1)dt_1}{\sqrt{(t-t_1)^2-\xi_1^2-(x-x_1)^2}} - \frac{1}{\pi}\int_0^{x+\sqrt{t^2-\xi_1^2}} dx_1 \int_0^{t-\sqrt{(x-x_1)^2+\xi_1^2}} \frac{w_u(x_1+Mt_1,y_1)dt_1}{\sqrt{(t-t_1)^2-\xi_1^2-(x-x_1)^2}} \tag{A2}$$

where

$$X_1(\xi_1)=\frac{M}{\beta}\left(x_m-\sqrt{t_m^2-\xi_1^2}\right)$$

With the values of W given in equations (A1) and (A2) it is possible now to solve equation (6b) for ψ, figure 8 giving the required data in the ξ,y plane. Thus, if $R^2=(\xi-\xi_1)^2-(y-y_1)^2$

$$\begin{aligned}\psi(\xi,x,y,t)=&-\frac{1}{\pi}\int_{\xi+y-t}^{y} dy_1\int_{\xi+(y-y_1)}^{t} d\xi_1\,\frac{W_A}{R}-\frac{1}{\pi}\int_{y}^{-\xi+y+t} dy_1\int_{\xi-(y-y_1)}^{t} d\xi_1\,\frac{W_A}{R}-\frac{1}{\pi}\int_{\xi+y-\sqrt{t^2-x^2}}^{y} dy_1\int_{\xi+(y-y_1)}^{\sqrt{t^2-x^2}} d\xi_1\,\frac{W_B-W_A}{R}-\\ &\frac{1}{\pi}\int_{y}^{-\xi+y+\sqrt{t^2-x^2}} dy_1\int_{\xi-(y-y_1)}^{\sqrt{t^2-x^2}} d\xi_1\,\frac{W_B-W_A}{R}+\frac{1}{\pi}\int_{\xi+y-t}^{0} dy_1\int_{\xi+(y-y_1)}^{t} d\xi_1\,\frac{W_A}{R}+\frac{1}{\pi}\int_{0}^{-\xi+t-y} dy_1\int_{\xi+(y+y_1)}^{t} d\xi_1\,\frac{W_A}{R}+\\ &\frac{1}{\pi}\int_{\xi+y-\sqrt{t^2-x^2}}^{0} dy_1\int_{\xi+(y-y_1)}^{\sqrt{t^2-x^2}} d\xi_1\,\frac{W_B-W_A}{R}+\frac{1}{\pi}\int_{0}^{-\xi-y+\sqrt{t^2-x^2}} dy_1\int_{\xi+(y+y_1)}^{\sqrt{t^2-x^2}} d\xi_1\,\frac{W_B-W_A}{R}\end{aligned} \tag{A3}$$

Now apply the operation of equation (7) and the potential φ_{V_a} is given by

$$\begin{aligned}\varphi_{V_a}=-\frac{1}{\pi}\Bigg\{&\int_{y-t}^{y} dy_1\,\bar{\int}_{y-y_1}^{t} d\xi_1\,\frac{\xi_1 W_A}{R_1^3}+\int_{y}^{y+t} dy_1\,\bar{\int}_{-(y-y_1)}^{t} d\xi_1\,\frac{\xi_1 W_A}{R_1^3}+\int_{y-\sqrt{t^2-x^2}}^{y} dy_1\,\bar{\int}_{y-y_1}^{\sqrt{t^2-x^2}} d\xi_1\,\frac{\xi_1(W_B-W_A)}{R_1^3}+\\ &\int_{y}^{y+\sqrt{t^2-x^2}} dy_1\,\bar{\int}_{-(y-y_1)}^{\sqrt{t^2-x^2}} d\xi_1\,\frac{\xi_1(W_B-W_A)}{R_1^3}-\int_{y-t}^{0} dy_1\,\bar{\int}_{y-y_1}^{t} d\xi_1\,\frac{\xi_1 W_A}{R_1^3}-\int_{y-\sqrt{t^2-x^2}}^{0} dy_1\,\bar{\int}_{y-y_1}^{\sqrt{t^2-x^2}} d\xi_1\,\frac{\xi_1(W_B-W_A)}{R_1^3}+\int_{0}^{t-y} dy_1\,\frac{W_A|_{\xi_1=y+y_1}}{\sqrt{4yy_1}}-\\ &\int_{0}^{t-y} dy_1\int_{y+y_1}^{t} d\xi_1\,\frac{\xi_1 W_A}{R_1^3}+\int_{0}^{\sqrt{t^2-x^2}-y} dy_1\,\frac{(W_B-W_A)|_{\xi_1=y+y_1}}{\sqrt{4yy_1}}-\int_{0}^{\sqrt{t^2-x^2}-y} dy_1\int_{y+y_1}^{\sqrt{t^2-x^2}} d\xi_1\,\frac{\xi_1(W_B-W_A)}{R_1^3}\Bigg\}\end{aligned} \tag{A4}$$

where $R_1^2=\xi_1^2-(y-y_1)^2$ and the bars on the integrals signify that the finite part of the integral is to be taken in the sense defined [1] in reference 10 and that the order of integration cannot, in general, be reversed.[2]

For convenience set

$$\varphi_{V_a}=-\frac{1}{\pi}\sum_{1}^{10} I_n \tag{A5}$$

where I_n is the nth integral group on the right-hand side of equation (A4).

Consider the first of these integral sets. Using equation (A1), we can write

$$I_1=\int_{y-t}^{y} dy_1\,\bar{\int}_{y-y_1}^{t} \frac{\xi_1 d\xi_1}{[\xi_1^2-(y-y_1)^2]^{3/2}}\int_{x-\sqrt{t^2-\xi_1^2}}^{x+\sqrt{t^2-\xi_1^2}} dx_1 \int_0^{t-\sqrt{(x-x_1)^2+\xi_1^2}} \frac{w_u(x_1+Mt_1,y_1)dt_1}{\sqrt{(t-t_1)^2-(x-x_1)^2-\xi_1^2}}$$

In order to simplify this expression, the order of these integrals will be rearranged so the integration with respect to ξ_1 can be carried out first. The technique of changing the order of repeated integrals with strong singularities set forth in reference 10 will be used here. Consider the change of order in the ξ_1,x_1 plane. Pretend for the moment, that the t_1 integration has been carried out. Then the highest order singularity (since w_u is bounded) in the ξ_1, x_1 plane has the order 3/2 which is weak in the sense that no residual occurs

[1] For the subsequent analysis to hold, the definition of the finite part given in reference 10 is essential. This definition differs from that given by Hadamard when it applies to multiple integrals.

[2] Since the order of integration plays an important role in the following development, integration first with respect to x and then with respect to y will be denoted $\int dy \int dx\, f(x,y)$ while integration first with respect to y and then with respect to x will be denoted $\int dx \int dy\, (x,y)$. When the notation $\int\int f(x,y)\,dydx$ is used, the order of integration is immaterial.

when the sequence of integration is reversed. The top of figure 15 shows the area of integration, so immediately

$$I_1=\int_{y-t}^{y} dy_1 \int_{x-\sqrt{t^2-(y-y_1)^2}}^{x+\sqrt{t^2-(y-y_1)^2}} dx_1 \int_{y-y_1}^{\sqrt{t^2-(x-x_1)^2}} \frac{\xi_1 d\xi_1}{[\xi_1^2-(y-y_1)^2]^{3/2}} \int_0^{t-\sqrt{(x-x_1)^2+\xi_1^2}} \frac{w_u(x_1+Mt_1,y_1)dt_1}{\sqrt{(t-t_1)^2-(x-x_1)^2-\xi_1^2}}$$

To change order in the ξ_1, t_1 plane, consult the bottom of figure 15. In this case an inherent singularity exists at the confluence of the singularity lines of the integrand; namely, where $\xi_1=y-y_1$ and $t_1=t-\sqrt{(x-x)_1^2+\xi_1^2}$. The change of order can therefore not be performed directly, but account must be taken of the existence of a residual term (see ref. 10). This residual is defined as the difference between the two integrals taken in different orders over a vanishingly small region surrounding the inherent singularity (the dotted region in bottom of figure 15). The residual R_t is then,

$$R_t=\lim_{\epsilon\to 0}\left\{\int_{y-y_1}^{\sqrt{(r_0+\epsilon)^2-(x-x_1)^2}} \frac{\xi_1 d\xi_1}{[\xi_1^2-(y-y_1)^2]^{3/2}} \int_{t-r_0-\epsilon}^{t-\sqrt{(x-x_1)^2+\xi_1^2}} \frac{w_u(x_1+Mt_1,y_1)dt_1}{\sqrt{(t-t_1)^2-(x-x_1)^2-\xi_1^2}} - \int_{t-r_0-\epsilon}^{t-r_0} w_u(x_1+Mt_1,y_1)dt_1 \int_{y-y_1}^{\sqrt{(t-t_1)^2-(x-x_1)^2}} \frac{\xi_1 d\xi_1}{[\xi_1^2-(y-y_1)^2]^{3/2}\sqrt{(t-t_1)^2-(x-x_1)^2-\xi_1^2}}\right\}$$

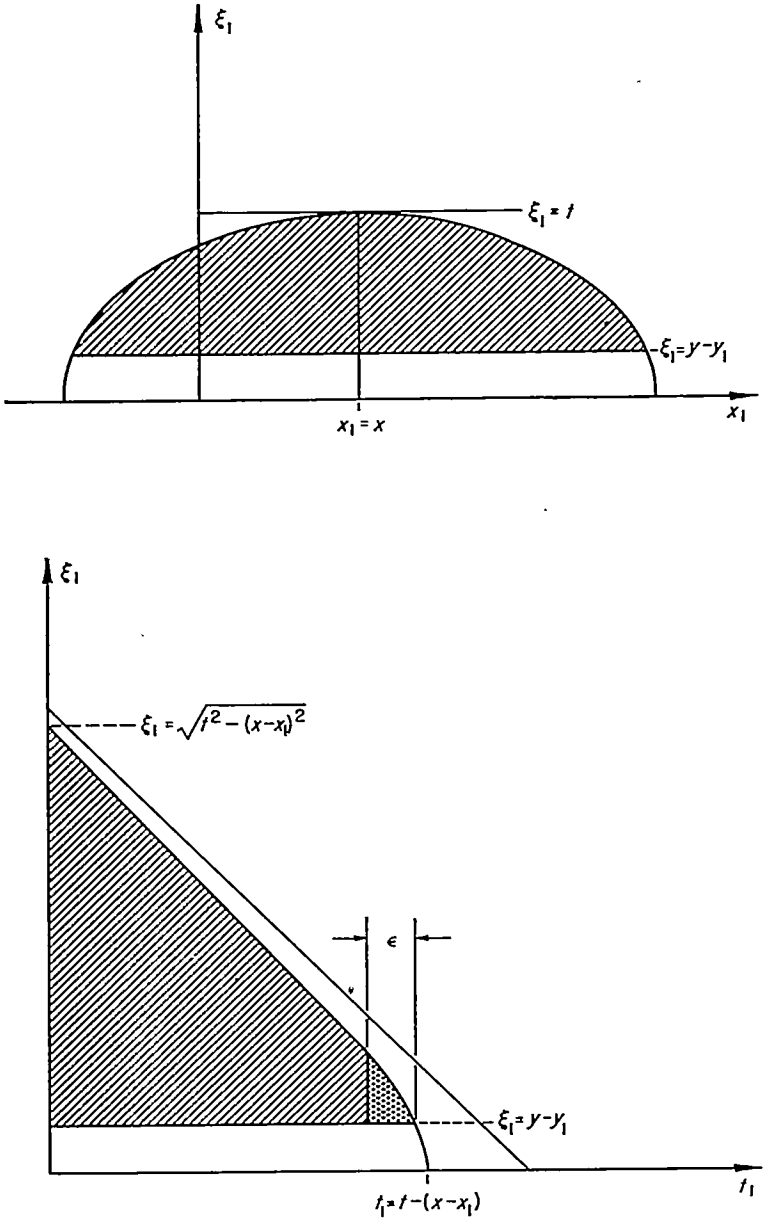

FIGURE 15.—Areas of integration used in analysis.

where $r_0^2=(x-x_1)^2+(y-y_1)^2$. The second integral vanishes (see ref. 10), and, passing to the limit $\epsilon\to 0$ in the first integral there results

$$R_t=-\frac{\pi}{2}\frac{w_u(x_1+Mt-Mr_0,y_1)}{r_0}=-\frac{\pi}{2}\frac{[w_u]}{r_0}$$

where the square brackets again mean that the retarded value is to be taken. Thus, the integral I_1 can be reduced to

$$I_1=-\frac{\pi}{2}\int_{y-t}^{y} dy_1 \int_{x-\sqrt{t^2-(y-y_1)^2}}^{x+\sqrt{t^2-(y-y_1)^2}} dx_1 \frac{[w_u]}{r_0} \tag{A6}$$

In the same way, the integral I_2 can be reduced, and

$$I_1+I_2=-\frac{\pi}{2}\int_{y-t}^{y+t} dy_1 \int_{x-\sqrt{t^2-(y-y_1)^2}}^{x+\sqrt{t^2-(y-y_1)^2}} dx_1 \frac{[w_u]}{r_0}$$

which is recognized as Kirchhoff's formula, equation (3), with an acoustic plan form bounded by the circle

$$(x-x_1)^2+(y-y_1)^2=t^2$$

The reduction of the integrals I_3, I_4, I_5, and I_6 is quite similar, leading to the sum

$$\sum_1^6 I_n=-\frac{1}{2\pi}\int_0^{y+t} dy_1 \int_{x-\sqrt{t^2-(y-y_1)^2}}^{x+\sqrt{t^2-(y-y_1)^2}} dx_1 \frac{[w_u]}{r_0} - \frac{1}{2\pi}\int_0^{y+\sqrt{t^2-x^2}} dy_1 \int_{X_1(y-y_1)}^{0} dx_1 \frac{[w_u]}{r_0} + \frac{1}{2\pi}\int_0^{y+\sqrt{t^2-x^2}} dy_1 \int_{x-\sqrt{t^2-(y-y_1)^2}}^{0} dx_1 \frac{[w_u]}{r_0} \tag{A7}$$

Examination of the limits on these integrals shows their total area of integration is that shown in figure 11. But this area corresponds exactly to the acoustic plan form S_a for a point in region V_a! Hence, denoting the combination of terms in equation (A7) by $\varphi^{(1)}$ we can write simply

$$\varphi^{(1)}_{V_a}=-\frac{1}{2\pi}\iint_{(S_a)V_a}\frac{[w_u]}{r_0}dx_1dy_1 \tag{A8}$$

It now remains to calculate the integrals I_7 through I_{10}. Designating their total effect on the potential, $\varphi^{(2)}$ one can readily show (since no inherent singularities arise in these cases) that

$$\varphi^{(2)}_{V_a}=\frac{1}{\pi^2}\int_0^{-y+t}dy_1\int_{x-\sqrt{t^2-(y+y_1)^2}}^{x+\sqrt{t^2-(y+y_1)^2}}dx_1\int_0^{t-r_1}\frac{\sqrt{4yy_1}\,w_u(x_1+Mt_1,y_1)dt_1}{[(t-t_1)^2-r_0^2]\sqrt{(t-t_1)^2-r_1^2}}-\frac{1}{\pi^2}\int_0^{-y+\sqrt{t^2-x^2}}dy_1\int_{x-\sqrt{t^2-(y+y_1)^2}}^{0}dx_1$$

$$\int_0^{t-r_1}\frac{\sqrt{4yy_1}\,w_u(x_1+Mt_1,y_1)dt_1}{[(t-t_1)^2-r_0^2]\sqrt{(t-t_1)^2-r_1^2}}+\frac{1}{\pi^2}\int_0^{-y+\sqrt{t^2-x^2}}dy_1\int_{X_1(y+y_1)}^{0}dx_1\int_{-x_1/M}^{t-r_1}\frac{\sqrt{4yy_1}\,w_u(x_1+Mt_1,y_1)dt_1}{[(t-t_1)^2-r_0^2]\sqrt{(t-t_1)^2-r_1^2}} \tag{A9}$$

where $r_1^2=(x-x_1)^2+(y+y_1)^2$. Now let

$$C(x_1,y_1)=\left\{\begin{array}{l}\displaystyle\int_{-x_1/M}^{t-r_1}\frac{\sqrt{4yy_1}\,w_u(x_1+Mt_1,y_1)\,dt_1}{[(t-t_1)^2-r_0^2]\sqrt{(t-t_1)^2-r_1^2}},\ x_1<0\\[2ex]\displaystyle\int_0^{t-r_1}\frac{\sqrt{4yy_1}\,w_u(x_1+Mt_1,y_1)\,dt_1}{[(t-t_1)^2-r_0^2]\sqrt{(t-t_1)^2-r_1^2}},\ x_1>0\end{array}\right\} \tag{A10}$$

In terms of this expression, equation (A9) can be written simply

$$\varphi^{(2)}_{V_a}=\frac{1}{\pi^2}\iint_{(S_c)_{V_a}}C(x_1,y_1)\,dx_1dy_1 \tag{A11}$$

where the area $(S_c)_{V_a}$ is illustrated in figure 12.

In order to give expressions for the potential in every region of the wing shown in figure 4, one can show that it is only necessary to vary the areas over which the double integration in equations (A8) and (A11) are carried out. This is evident in connection with the source portion $\varphi^{(1)}$, for in every case

$$\varphi^{(1)}=-\frac{1}{2\pi}\iint_{S_a}\frac{[w_u]}{r_0}\,dx_1dy_1 \tag{A12}$$

and only the acoustic plan form S_a changes with the region. In the case of $\varphi^{(2)}$, the part of the potential due to the existence of the side edge of the wing, equation (A11) can be generalized and written

$$\varphi^{(2)}=\frac{1}{\pi^2}\iint_{S_c}C(x_1,y_1)\,dx_1dy_1 \tag{A13}$$

where the integrands are defined in every case by equation (A10) and only the "reflected" acoustic plan form S_c changes with the region. The region S_c is always bounded by portions of the "reflected" circle

$$(x-x_1)^2+(y+y_1)^2=t^2$$

and the "reflected" ellipse

$$\left(\frac{\beta}{M}x_1-x_m\right)^2+(y+y_1)^2=t_m^2$$

Figure 16 shows sketches of both S_c and S_a for all regions in figure 4. The absence of a sketch indicates that the corresponding integral does not exist for that region.

APPENDIX B

THE GENERALIZED INDICIAL FORCES

THE LOADING COEFFICIENT

In order to determine total forces acting on the wing, it is first necessary to obtain expressions for the loading coefficient $\Delta p/q_0$. According to the linear theory

$$\frac{\Delta p}{q_0}=\frac{4}{U_0M}\frac{\partial\varphi}{\partial t} \tag{B1}$$

so it is necessary to differentiate each of the expressions for potential. As an example, consider, as in Appendix A, just region V_a of figure 4. The loading coefficient will be divided into two parts $\Delta p^{(1)}/q_0$ and $\Delta p^{(2)}/q_0$ to correspond to the potentials $\varphi^{(1)}$ and $\varphi^{(2)}$. Thus, using equation (A11)

$$\left(\frac{\Delta p}{q_0}\right)\Big|^{(2)}_{V_a}=\frac{4}{\pi^2U_0M}\left\{\int_0^{-y+t}dy_1\int_{x-\sqrt{t^2-(y+y_1)^2}}^{x+\sqrt{t^2-(y+y_1)^2}}\frac{\partial C}{\partial t}\,dx_1-\right.$$

$$\int_0^{-y+\sqrt{t^2-x^2}}dy_1\int_{x-\sqrt{t^2-(y+y_1)^2}}^{0}\frac{\partial C}{\partial t}\,dx_1+$$

$$\left.\int_0^{-y+\sqrt{t^2-x^2}}dy_1\int_{X_1(y+y_1)}^{0}\frac{\partial C}{\partial t}\,dx_1\right\} \tag{B2}$$

since the derivative passes the x_1,y_1 integration without effect. Referring to equation (A10) for the function $C(x_1,y_1)$ we next find its derivative with respect to t. Write $\tau=t-t_1$; then for $x_1<0$

$$C(x_1,y_1)=\int_{r_1}^{t+x_1/M}\frac{\sqrt{4yy_1}\,w_u(x_1+Mt-M\tau,y_1)d\tau}{(\tau^2-r_0^2)\sqrt{\tau^2-r_1^2}}$$

and

$$\frac{\partial C}{\partial t}=\frac{\sqrt{4yy_1}\,w_u(0,y)}{\left[\left(t+\frac{x_1}{M}\right)^2-r_0^2\right]\sqrt{\left(t+\frac{x_1}{M}\right)^2-r_1^2}}+$$

$$\int_{r_1}^{t+x_1/M}\frac{\sqrt{4yy_1}\,\frac{\partial}{\partial t}\left\{w_u(x_1+Mt-M\tau,y_1)\right\}}{(\tau^2-r_0^2)\sqrt{\tau^2-r_1^2}}\,d\tau \tag{B3}$$

Notice that if w_u does not depend on (x_1+Mt_1) the integral term in equation (B3) vanishes, while if it does, then the integrated term is zero. Next, for $x_1>0$,

$$C(x_1,y_1)=\int_{r_1}^{t}\frac{\sqrt{4yy_1}\,w_u(x_1+Mt-M\tau,y_1)}{(\tau^2-r_0^2)\sqrt{\tau^2-r_1^2}}\,d\tau$$

and

$$\frac{\partial C}{\partial t}=\frac{\sqrt{4yy_1}\,w_u(x_1,y_1)}{(t^2-r_0^2)\sqrt{t^2-r_1^2}}+\int_{r_1}^{t}\frac{\sqrt{4yy_1}\,\frac{\partial}{\partial t}\left\{w_u(x_1+Mt-M\tau,y_1)\right\}}{(\tau^2-r_0^2)\sqrt{\tau^2-r_1^2}}\,d\tau \tag{B4}$$

In this case, both terms exist unless w_u is not a function of (x_1+Mt_1), in which case the integral vanishes.

Substitution of equations (B3) and (B4) into equation (B2) will now yield an expression for the loading coefficient corresponding to the influence of the side edge;

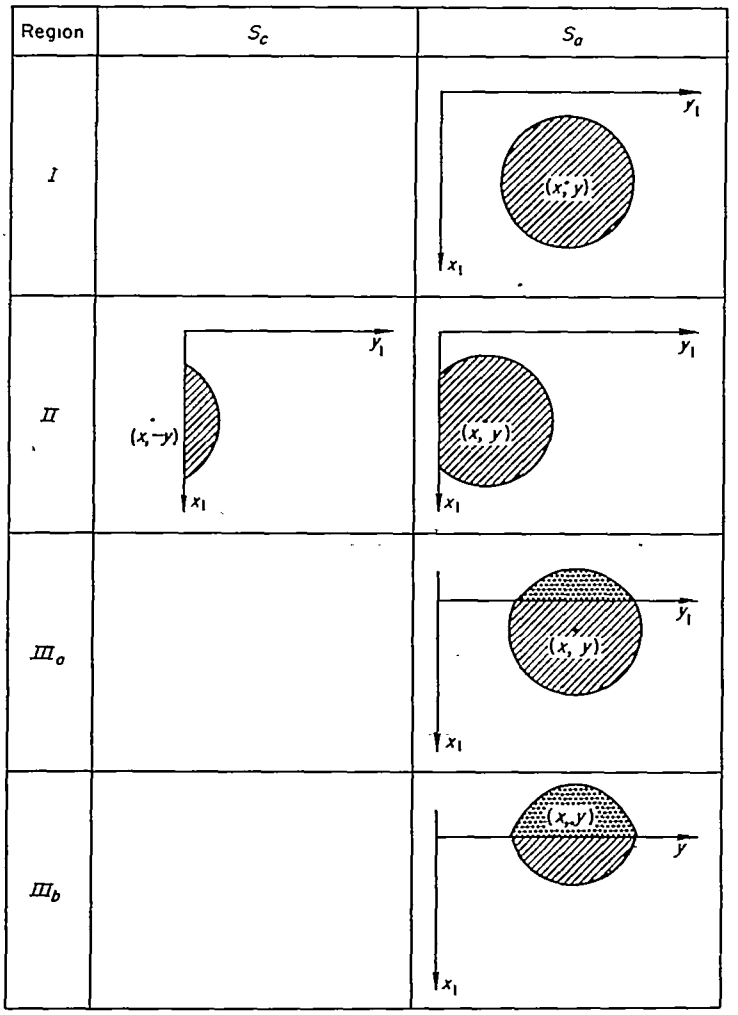

FIGURE 16.—Sketches of areas of integration, S_c and S_a, for all regions in figure 4.

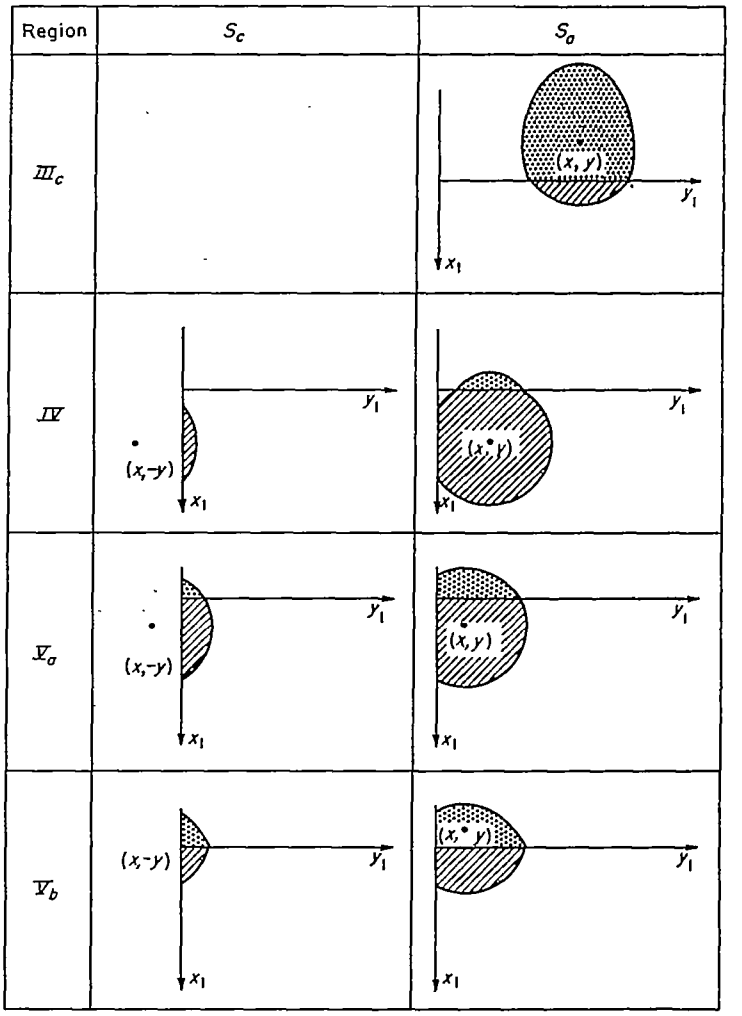

FIGURE 16—Continued

$$\left(\frac{\Delta p}{q_0}\right)\Big|_{V_a}^{(2)}=\frac{4a_{ln}}{\pi^2 U_0 M c^{l+n}}\left\{\int_0^{-y+t} dy_1 \int_{x-\sqrt{t^2-(y+y_1)^2}}^{x+\sqrt{t^2-(y+y_1)^2}} \frac{\sqrt{4yy_1}\, x_1^{\,l} y_1^{\,n} dx_1}{(t^2-r_0^2)\sqrt{t^2-r_1^2}} + Ml \int_0^{-y+t} dy_1 \int_{x-\sqrt{t^2-(y+y_1)^2}}^{x+\sqrt{t^2-(y+y_1)^2}} dx_1 \int_0^{t-r_1} \frac{\sqrt{4yy_1}\,(x_1+Mt_1)^{l-1} y_1^{\,n} dt_1}{[(t-t_1)^2-r_0^2]\sqrt{(t-t_1)^2-r_1^2}} - \right.$$

$$\int_{-y+\sqrt{t^2-x^2}}^{-y+t} dy_1 \int_{x-\sqrt{t^2-(y+y_1)^2}}^{0} \frac{\sqrt{4yy_1}\, x_1^{\,l} y_1^{\,n} dx_1}{(t^2-r_0^2)\sqrt{t^2-r_1^2}} - Ml \int_0^{-y+\sqrt{t^2-x^2}} dy_1 \int_{x-\sqrt{t^2-(y+y_1)^2}}^{0} dx_1 \int_0^{t-r_1} \frac{\sqrt{4yy_1}\,(x_1+Mt_1)^{l-1} y_1^{\,n} dt_1}{[(t-t_1)^2-r_0^2]\sqrt{(t-t_1)^2-r_1^2}} +$$

$$\left. Ml \int_0^{-y+\sqrt{t^2-x^2}} dy_1 \int_{X_1(y+y_1)}^{0} dx_1 \int_{-(x_1/M)}^{t-r_1} \frac{\sqrt{4yy_1}\,(x_1+Mt_1)^{l-1} y_1^{\,n} dt_1}{[(t-t_1)^2-r_0^2]\sqrt{(t-t_1)^2-r_1^2}} \right\} \tag{B5}$$

The explicit form of w_u, given by equation (2), has been inserted and it is assumed that $l \geq 1$.

The portion of the loading coefficient corresponding to $\varphi_{V_a}^{(1)}$ can be found readily and is

$$\left(\frac{\Delta p}{q_0}\right)\Big|_{V_a}^{(1)}=-\frac{2a_{ln}}{\pi M U_0 c^{l+n}}\left\{\int_0^{y+t} y_1^{\,n} \frac{\left(x+\sqrt{t^2-(y-y_1)^2}\right)^l+\left(x-\sqrt{t^2-(y-y_1)^2}\right)^l}{\sqrt{t^2-(y-y_1)^2}}\, dy_1 + \right.$$

$$Ml \int_0^{y+t} y_1^{\,n} dy_1 \int_{x-\sqrt{t^2-(y-y_1)^2}}^{x+\sqrt{t^2-(y-y_1)^2}} \frac{[x_1+M(t-r_0)]^{l-1}}{r_0}\, dx_1 -$$

$$Ml \int_0^{y+\sqrt{t^2-x^2}} y_1^{\,n} dy_1 \int_{x-\sqrt{t^2-(y-y_1)^2}}^{0} \frac{[x_1+M(t-r_0)]^{l-1}}{r_0}\, dx_1 +$$

$$Ml \int_0^{y+\sqrt{t^2-x^2}} y_1^{\,n} dy_1 \int_{X_1(y-y_1)}^{0} \frac{[x_1+M(t-r_0)]^{l-1}}{r_0}\, dx_1 -$$

$$\left. \int_0^{y+\sqrt{t^2-x^2}} y_1^{\,n} \frac{\left(x-\sqrt{t^2-(y-y_1)^2}\right)^l}{\sqrt{t^2-(y-y_1)^2}}\, dy_1 \right\} \tag{B6}$$

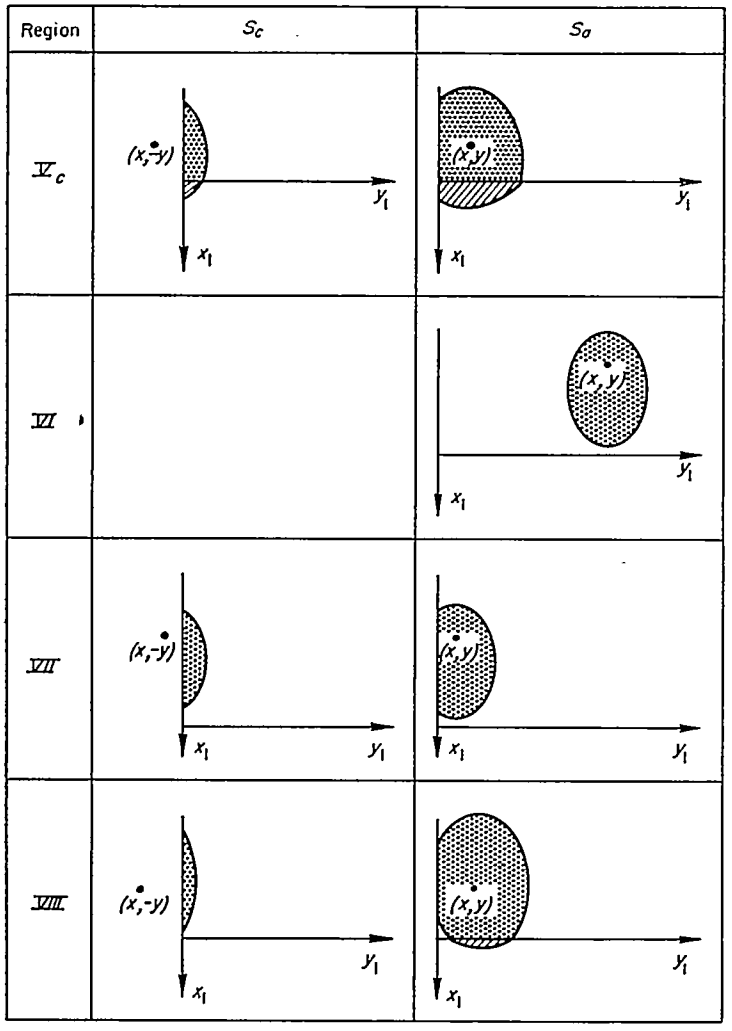

FIGURE 16—Concluded

It is clear that, even for small values of the indices l and n, the required integrations for the determination of total forces on the wing pose formidable problems. There is, however, a property of the loading coefficient corresponding to vertical velocity distributions of the type chosen here (eq. (2)) that will materially shorten the requisite labor. This may be expressed as follows, adopting the convention that $\Delta p^{ln}/q_0$ corresponds to a downwash distribution proportional to $(x+Mt)^l y^n$:

$$\frac{\partial}{\partial x}\frac{\Delta p^{ln}}{q_0}=\frac{l}{c}\frac{\Delta p^{l-1,n}}{q_0}, \quad l>0 \tag{B7}$$

or

$$\frac{\Delta p^{ln}}{q_0}=\frac{l}{c}\int_{-Mt}^{x}\frac{\Delta p^{l-1,n}}{q_0}(x_1,y,t)\,dx_1, \quad l>0 \tag{B8}$$

DETAILS OF EVALUATING THE GENERALIZED INDICIAL FORCES

In calculating the generalized indicial forces by means of equation (36), it has been shown that only the value zero need be taken for the index l. Thus we must find

$$F^{0n}_{jg}=\frac{2}{bc^{j+g+1}}\int_{-Mt}^{c-Mt}(x+Mt)^j dx\int_0^s y^g\frac{\Delta p^{0n}}{q_0}\,dy \tag{B9}$$

The values of the loading coefficient $\Delta p^{0n}/q_0$ are found by differentiating the expressions for potential given in the first part of this appendix.

It is convenient, in evaluating equation (B9), to consider the integration with respect to y first. Setting

$$L=\int_0^s\left(\frac{y}{c}\right)^g\frac{\Delta p^{0n}}{q_0}\,dy \tag{B10}$$

it is found that L seems to have different representations according to the interval in which x lies. These expressions can, however, all be expressed by the same formula. The portions of L corresponding to the parts $\varphi^{(1)}$ and $\varphi^{(2)}$ of the potential are similarly signified, and we have

$$L^{(1)}=\frac{2a_{0n}}{\pi U_0 M c^{n+g}}\left\{(-1)^n\frac{n!g!}{(n+g+1)!}[K_0(n+g)+K_M(n+g)]-\right.$$
$$\left.2\sum_{\mu=0}^{[n/2]}\binom{n}{2\mu}\frac{(g)^{n+g+1-2\mu}}{n+g+1-2\mu}[K_0(2\mu-1)+K_M(2\mu-1)]\right\} \tag{B11}$$

$$L^{(2)}=\frac{a_{0n}}{\pi U_0 M c^{n+g}}\frac{J(n,g)}{2^{n+g}}[K_0(n+g)+K_M(n+g)] \tag{B12}$$

where

$$K_0(n+g)=t^{n+g+1}R.P.\int_0^{\cos^{-1}(-x/t)}\sin^{n+g+1}\theta d\theta$$

$$K_M(n+g)=\frac{M}{\beta}t_m^{n+g+1}R.P.\int_0^{\cos^{-1}(x_m/t_m)}\sin^{n+g+1}\theta d\theta$$

$$J(n,g)=\frac{2}{\pi}\int_0^1\frac{d\eta}{\sqrt{1-\eta^2}}\int_{-\eta}^{\eta}\frac{(\eta-\eta_1)^g(\eta+\eta_1)^n}{1-\eta_1^2}\sqrt{\eta^2-\eta_1^2}\,d\eta_1$$

and $[n/2]$ means the greatest integer contained in $n/2$. The function $J(n,g)$ may be expressed as summations, and it has the property

$$J(n,g)=J(g,n) \tag{B13}$$

The sum formula is, with $g+p=n$

$$J(g,n)=(-1)^g\sum_{i=0}^{[p/2]}\binom{p}{2i}\left[B\left(\frac{p-2i+1}{2},\frac{2g+1}{2}\right)-\right.$$
$$\left.B\left(\frac{p-2i+1}{2};\frac{2g+2}{2}\right)\right]+\frac{(-1)^{g-1}}{\pi}\sum_{i=0}^{[p/2]}\binom{p}{2i}\sum_{j=0}^{g-1}(-1)^j$$
$$B\left(\frac{2j+3}{2},\frac{1}{2}\right)B\left(\frac{p-2i+2j+3}{2},\frac{2g-2j-1}{2}\right)-\frac{1}{\pi}\sum_{i=0}^{[p/2]}$$
$$\binom{p}{2i}\sum_{i=0}^{-1}B\left(\frac{2j+1}{2},\frac{2g+3}{2}\right)B\left(\frac{p+2g-2i+2j+3}{2},\frac{1}{2}\right) \tag{B14}$$

Values of the function $J(g,n)$

g \ n	0	1	2	3	4	5
0	$\pi-2$					
1	1	$-\frac{1}{4}\pi+\frac{4}{3}$				
2	$\frac{5}{4}\pi-\frac{8}{3}$	$\frac{1}{2}$	$\frac{29}{64}\pi-\frac{16}{15}$			
3	$\frac{11}{6}$	$-\frac{21}{64}\pi+\frac{8}{5}$	$\frac{1}{3}$	$-\frac{53}{256}\pi+\frac{32}{35}$		
4	$\frac{189}{64}\pi-\frac{32}{5}$	$\frac{11}{15}$	$\frac{129}{256}\pi-\frac{128}{105}$	$\frac{1}{4}$	$\frac{5329}{16384}\pi-\frac{256}{315}$	
5	$\frac{71}{15}$	$-\frac{165}{256}\pi+\frac{64}{21}$	$\frac{37}{84}$	$-\frac{975}{4096}\pi+\frac{64}{63}$	$\frac{1}{5}$	$-\frac{11801}{65536}\pi+\frac{512}{693}$

where $\binom{p}{2i}$ is the binomial coefficient

$$\binom{p}{2i}=\frac{p!}{(2i)!(p-2i)!}$$

and $B(p, q)$ is the beta function

$$\left.\begin{aligned} B(p,q)&=\int_0^1 x^{p-1}(1-x)^{q-1}dx \\ &=2\int_0^{\pi/2}\sin^{2p-1}\theta\cos^{2q-1}\theta d\theta \\ &=\Gamma(p)\Gamma(q)/\Gamma(p+q) \end{aligned}\right\} \qquad \text{(B15a)}$$

The function $J(g, n)$ has been calculated for g, n taken 0, 1, 2, 3, 4, 5. Because of the property (B13), it is only necessary to give a triangular array, which appears in the above table.

Now consider the functions $K_0(\nu)$ and $K_M(\nu)$, defined after equation (B12). It is convenient, for computational purposes, to express these in terms of the incomplete beta functions, defined as

$$\left.\begin{aligned} B_{1-x^2}(p,q)&=2\int_0^{\cos^{-1}(x)}\sin^{2p-1}\theta\cos^{2q-1}\theta d\theta \\ &=\int_0^{1-x^2}\xi^{p-1}(1-\xi)^{q-1}d\xi \end{aligned}\right\} \qquad \text{(B15b)}$$

A tabulation of the incomplete beta functions is available in reference 11. Note that when the symbol B is written without a subscript, the complete integral is meant, that is, in equation (B15b), x equals 0. It is necessary to exercise some care when interpreting $K_0(\nu)$ and $K_M(\nu)$ as beta functions because of the upper limit. Thus, since

$$K_0(\nu)=t^{\nu+1}R.P.\int_0^{\cos^{-1}(-x/t)}\sin^{\nu+1}\theta d\theta$$

we have the following cases:

(i) $x\geq t$, $R.P.\cos^{-1}\left(-\frac{x}{t}\right)=\pi$

$$K_0(\nu)=t^{\nu+1}B\left(\frac{\nu+2}{2},\frac{1}{2}\right)$$

(ii) $0\leq x\leq t$, $R.P.\cos^{-1}\left(-\frac{x}{t}\right)=\cos^{-1}\left(-\frac{x}{t}\right)=\pi-\cos^{-1}\left(\frac{x}{t}\right)$

$$K_0(\nu)=\frac{t^{\nu+1}}{2}\left[2B\left(\frac{\nu+2}{2},\frac{1}{2}\right)-B_{1-(x/t)^2}\left(\frac{\nu+2}{2},\frac{1}{2}\right)\right]$$

(iii) $-t\leq x\leq 0$, $R.P.\cos^{-1}\left(-\frac{x}{t}\right)=\cos^{-1}\left(-\frac{x}{t}\right)$

$$K_0(\nu)=\frac{t^{\nu+1}}{2}\left[B_{1-(x/t)^2}\left(\frac{\nu+2}{2},\frac{1}{2}\right)\right]$$

(iv) $-Mt\leq x\leq -t$; $R.P.\cos^{-1}\left(-\frac{x}{t}\right)=0$

$$K_0(\nu)=0$$

A similar line taken with $K_M(\nu)$ leads to

(i) $x\geq t$, $K_M(\nu)=0$

(ii) $-\frac{t}{M}\leq x\leq t$, $K_M(\nu)=\frac{1}{2}\frac{M}{\beta}t_m^{\nu+1}\left[B_{1-(x_m/t_m)^2}\left(\frac{\nu+2}{2},\frac{1}{2}\right)\right]$

(iii) $-t\leq x\leq -\frac{t}{M}$, $K_M(\nu)=\frac{1}{2}\frac{M}{\beta}t_m^{\nu+1}\left[2B\left(\frac{\nu+2}{2},\frac{1}{2}\right)-B_{1-(x_m/t_m)^2}\left(\frac{\nu+2}{2},\frac{1}{2}\right)\right]$

(iv) $-Mt\leq x\leq -t$, $K_M(\nu)=\frac{M}{\beta}t_m^{\nu+1}B\left(\frac{\nu+2}{2},\frac{1}{2}\right)\Big]$

The generalized indicial force F_{jg}^{0n} can now be expressed as

$$F_{jg}^{0n}=\frac{8a_{0n}}{\pi MU_0c^{j+s+n+1}}\left\{\frac{1}{4}\left[\frac{J(g,n)}{2^{s+n}}+2(-1)^n\frac{n!g!}{(n+g+1)!}\right]\right.$$
$$\left[{}^*I_0^j(g+n)+{}^*I_M^j(g+n)\right]-\sum_{\mu=0}^{[n/2]}\binom{n}{2\mu}\frac{8^{s+n+1-2\mu}}{g+n+1-2\mu}$$
$$\left.\left[{}^*I_0^j(2\mu-1)+{}^*I_M^j(2\mu-1)\right]\right\} \qquad \text{(B16)}$$

where

$$*I_0^j(\nu)=\int_{-Mt}^{c-Mt}(x+Mt)^j dx\left[t^{\nu+1}R.P.\int_0^{\cos^{-1}(-x/t)}\sin^{\nu+1}\theta d\theta\right] \tag{B17}$$

$$*I_M^j(\nu)=\int_{-Mt}^{c-Mt}(x+Mt)^j dx\left[\frac{M}{\beta}t_m^{\nu+1}R.P.\int_0^{\cos^{-1}(x_m/t_m)}\sin^{\nu+1}\theta d\theta\right] \tag{B18}$$

It is convenient to express these forces in terms of dimensionless quantities. Thus setting

$$x_0=\frac{x}{c},\qquad t_0=\frac{t}{c}$$

we have

$$*I_0^j(\nu)=c^{j+\nu+2}\int_{-Mt_0}^{1-Mt_0}(x_0+Mt_0)^j dx_0\left[t_0^{\nu+1}R.P.\int_0^{\cos^{-1}(-x_0/t_0)}\sin^{\nu+1}\theta d\theta\right]=c^{j+\nu+2}I_0^j(\nu) \tag{B19}$$

$$*I_M^j(\nu)=c^{j+\nu+2}\int_{-Mt_0}^{1-Mt_0}(x_0+Mt_0)^j dx_0\left[\frac{M}{\beta}\left(\frac{x_0+Mt_0}{\beta}\right)^{\nu+1}R.P.\int_0^{\cos^{-1}\frac{Mx_0+t_0}{x_0+Mt_0}}\sin^{\nu+1}\theta d\theta\right]=c^{j+\nu+2}I_M^j(\nu) \tag{B20}$$

and

$$F_{jg}^{0n}=\frac{4a_{0n}}{\pi MU_0}\left\{\frac{1}{2A}\left[\frac{J(g,n)}{2^{g+n}}+(-1)^n 2\frac{n!g!}{(n+g+1)!}\right]\left[I_0^j(g+n)+I_M^j(g+n)\right]-\sum_{\mu=0}^{[n/2]}\binom{n}{2\mu}\frac{\left(\frac{A}{2}\right)^{g+n-2\mu}}{g+n+1-2\mu}\left[I_0^j(2\mu-1)+I_M^j(2\mu-1)\right]\right\} \tag{B21}$$

The integrals $I_0^j(\nu)$ and $I_M^j(\nu)$ can be simplified by reversing the order of integration. This can be accomplished in a straight-forward manner by merely inspecting the region of integration in the x_0,θ plane. Consider first the integral $I_0^j(\nu)$. Depending upon the relation between the chord length and the time, we see—from figure 17—that reversing the order of integration results in three different possibilities for the upper limit of the θ integral. However, if we define χ_0 such that

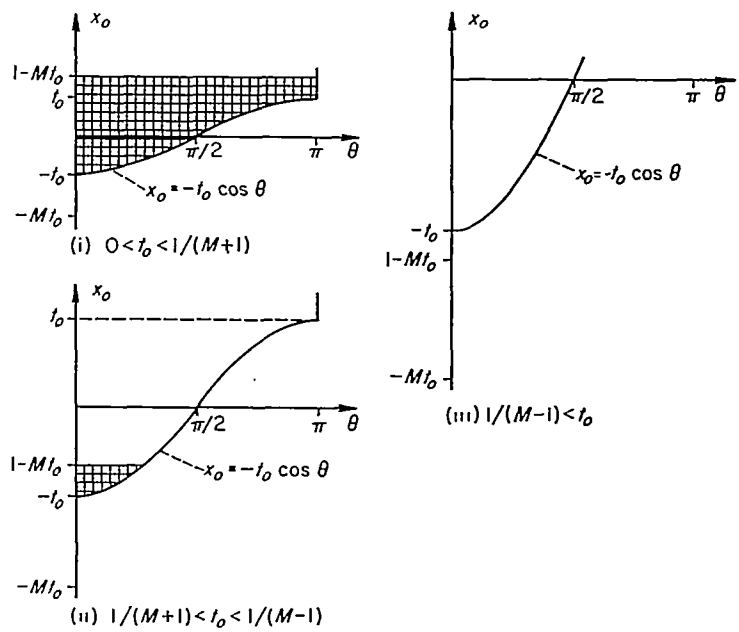

FIGURE 17.—Areas of integration used in analysis.

(i) $\chi_0=t_0;\ 0\le t_0\le\frac{1}{M+1}$

(ii) $\chi_0=1-Mt_0;\ \frac{1}{M+1}\le t_0\le\frac{1}{M-1}$

(iii) $\chi_0=-t_0;\ \frac{1}{M-1}\le t_0$

then, in every case, $I_0^j(\nu)$ can be written

$$I_0^j(\nu)=\frac{t_0^{\nu+1}}{j+1}\int_0^{\cos^{-1}(-\chi_0/t_0)}\sin^{\nu+1}\theta d\theta-\frac{t_0^{j+\nu+2}}{j+1}\sum_{r=0}^{j+1}(-1)^r\binom{j+1}{r}M^{j+1-r}\int_0^{\cos^{-1}(-\chi_0/t_0)}\sin^{\nu+1}\theta\cos^r\theta d\theta \tag{B22}$$

and, similarly, it can be shown that

$$I_M^j(\nu)=\frac{M}{\beta^{\nu+2}}\frac{1}{j+\nu+2}\int_0^{\cos^{-1}\frac{1+M\chi_0/t_0}{M+\chi_0/t_0}}\sin^{\nu+1}\theta d\theta+\frac{Mt_0^{j+\nu+2}}{j+\nu+2}\sum_{r=0}^{j}(-1)^r\binom{j}{r}M^{j-r}\int_0^{\cos^{-1}(-\chi_0/t_0)}\sin^{\nu+1}\theta\cos^r\theta d\theta \tag{B23}$$

APPENDIX C

DERIVATION OF RECIPROCITY RELATIONS

According to reference 5, the reciprocity relation for general three-dimensional unsteady motion can be written

$$\iiint_{V_1} \frac{\Delta p_1}{q_0}(x_1,y_1,t_1)W_2(x_1,y_1,t_1)\,dx_1dy_1dt_1 = \iiint_{V} \frac{\Delta p_2}{q_0}(x_2,y_2,t_2)W_1(x_2,y_2,t_2)\,dx_2dy_2dt_2 \quad \text{(C1)}$$

where the volume of integration V is that swept out in x, y, t space by the wing. The subscript 1 refers to the wing moving in the forward direction and subscript 2 refers to the wing moving in the opposite direction in the same manner. The coordinate systems are related by

$$x_1=-x_2+c-MT$$

$$y_1=-y_2+2s$$

$$t_1=-t_2+T$$

where s, c are wing semispan and chord, respectively, and T is some fixed value of time. These quantities are elucidated in figure 18.

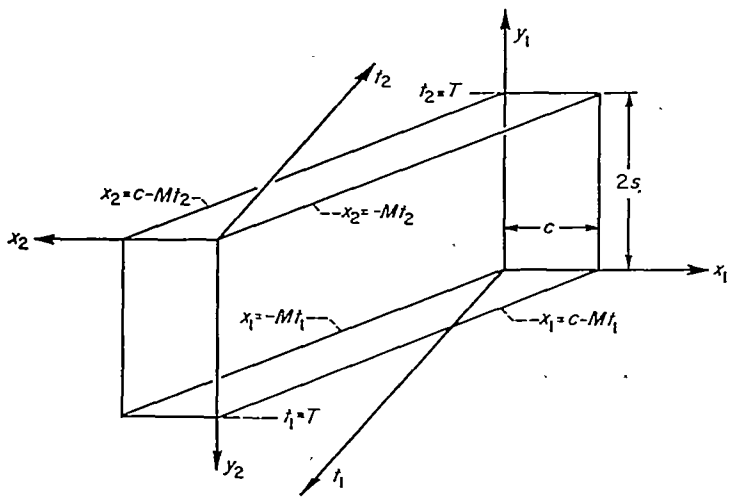

FIGURE 18.—Coordinate system in forward and reversed flow.

Now let the wing associated with the subscript 1 have the vertical velocity distribution

$$w_1(x_1,y_1,t_1)=\left(\frac{x_1+Mt_1}{c}\right)^l\left(\frac{s-y_1}{c}\right)^n$$

and that associated with the subscript 2 have

$$w_2(x_2,y_2,t_2)=\left(\frac{x_2+Mt_2}{c}\right)^j\left(\frac{s-y_2}{c}\right)^g$$

Then

$$w_1(x_2,y_2,t_2)=\left(1-\frac{x_2+Mt_2}{c}\right)^l\left(\frac{y_2-s}{c}\right)^n$$

$$w_2(x_1,y_1,t_1)=\left(1-\frac{x_1+Mt_1}{c}\right)^j\left(\frac{y_1-s}{c}\right)^g$$

Substitution of these results into equation (C1) yields

$$\int_0^T dt_1\int_{-Mt_1}^{c-Mt_1} dx_1\left(1-\frac{x_1+Mt_1}{c}\right)^j\int_0^{2s} dy_1\left(\frac{y_1-s}{c}\right)^g\frac{\Delta p^{ln}}{q_0} = \int_0^T dt_2\int_{-Mt_2}^{c-Mt_2} dx_2\left(1-\frac{x_2+Mt_2}{c}\right)^l\int_0^{2s} dy_2\left(\frac{y_2-s}{c}\right)^n\frac{\Delta p^{jg}}{q_0} \quad \text{(C2)}$$

Equation (C2) can be differentiated with respect to T, yielding

$$\int_{-MT}^{c-MT} dx_1\left(1-\frac{x_1+MT}{c}\right)^j\int_0^{2s} dy_1\left(\frac{y_1-s}{c}\right)^g\frac{\Delta p^{ln}}{q_0} = \int_{-MT}^{c-MT} dx_2\left(1-\frac{x_2+MT}{c}\right)^l\int_0^{2s} dy_2\left(\frac{y_2-s}{c}\right)^n\frac{\Delta p^{jg}}{q_0}$$

The binomial expansion is now performed:

$$\sum_{\mu=0}^{j}(-1)^\mu\binom{j}{\mu}(-1)^g\int_{-MT}^{c-MT} dx_1\left(\frac{x_1+MT}{c}\right)^\mu\int_0^{2s} dy_1\left(\frac{s-y_1}{c}\right)^g\frac{\Delta p^{ln}}{q_0} = \sum_{\mu=0}^{l}(-1)^\mu\binom{l}{\mu}(-1)^n\int_{-MT}^{c-MT} dx_2\left(\frac{x_2+MT}{c}\right)^\mu\int_0^{2s} dy_2\left(\frac{s-y_2}{c}\right)^n\frac{\Delta p^{jg}}{q_0} \quad \text{(C3)}$$

In equation (C3) the spanwise integration is carried over the whole wing, but it can easily be reduced to integration over, say, the left panel by use of the factor $[1+(-1)^{g+n}]/2$. Thus, equation (C3) can be written

$$(-1)^g\sum_{\mu=0}^{j}(-1)^\mu\binom{j}{\mu}\frac{[1+(-1)^{g+n}]/2}{sc}\int_{-MT}^{c-MT} dx_1\left(\frac{x_1+MT}{c}\right)^\mu \int_0^{s} dy_1\left(\frac{s-y_1}{c}\right)^g\frac{\Delta p^{ln}}{q_0} = (-1)^n\sum_{\mu=0}^{l}(-1)^\mu\binom{l}{\mu}\frac{[1+(-1)^{g+n}]/2}{sc} \int_{-MT}^{c-MT} dx_2\left(\frac{x_2+MT}{c}\right)^\mu\int_0^{s} dy_2\left(\frac{s-y_2}{c}\right)^n\frac{\Delta p^{jg}}{q_0}$$

By comparison with equations (36) and (37), it is seen that the integral terms in the last equation correspond to the generalized indicial forces $f_{\mu g}^{ln}$ and $f_{\mu n}^{jg}$, so that the summations can be written

$$\sum_{\mu=0}^{j}(-1)^\mu\binom{j}{\mu}f_{\mu g}^{ln}=\sum_{\mu=0}^{l}(-1)^\mu\binom{l}{\mu}f_{\mu n}^{jg} \quad \text{(C4)}$$

where the quantity $(g+n)$ must be an even number.

REFERENCES

1. Gardner, C.: Time-Dependent Linearized Supersonic Flow Past Planar Wings. Comm. Pure and Appl. Math., vol. III, no. 1, Mar. 1950, pp. 33–38.
2. Miles, John W.: Transient Loading of Supersonic Rectangular Airfoils. Jour. Aero. Sci., vol. 17, no. 10, Oct. 1950, pp. 647–652.
3. Miles, John W.: A General Solution For The Rectangular Airfoil in Supersonic Flow. Quart. Appl. Math., vol. XI, Apr. 1953, pp. 1–8.
4. Hadamard, Jacques Solomon: Lectures on Cauchy's Problem in Linear Partial Differential Equations. Yale Univ. Press, New Haven, Conn., 1923.

5. Heaslet, Max. A., and Spreiter, John R.: Reciprocity Relations in Aerodynamics. NACA Rep. 1119, 1953.

6. Lomax, Harvard, Heaslet, Max. A., Fuller, Franklyn B., and Sluder, Loma: Two- and Three-Dimensional Unsteady Lift Problems in High-Speed Flight. NACA Rep. 1077, 1952.

7. Baker, Bevan B., and Copson, E. T.: The Mathematical Theory of Huygens' Principle. The Clarendon Press, Oxford, England, 1939, pp. 54 ff.

8. Evvard, John C.: Use of Source Distributions For Evaluating Theoretical Aerodynamics of Thin Finite Wings at Supersonic Speeds. NACA Rep. 951, 1950.

9. Rayleigh, John William Strutt: The Theory of Sound, vol. I, Dover Pub., New York, 1945, p. 353.

10. Lomax, Harvard, Heaslet, Max. A., and Fuller, Franklyn B.: Integrals and Integral Equations in Linearized Wing Theory. NACA Rep. 1054, 1951.

11. Pearson, Karl: Tables of the Incomplete Beta-Function. Cambridge Univ. Press, Cambridge, England, 1948.

TABLE I.—VALUES OF GENERALIZED INDICIAL FORCES, F_{jg}^{ln}

The generalized indicial force coefficient F_{jg}^{ln} is defined by equation (36). It is the response for a mode shape having a unit amplitude

$$h_{mode}=\left(\frac{x+Mt}{c}\right)^{j}\left(\frac{y}{c}\right)^{g}$$

and a loading induced by a unit value of w/U_0,

$$\frac{w}{U_0}=-\left(\frac{x+Mt}{c}\right)^{l}\left(\frac{y}{c}\right)^{n}$$

The table gives values of F_{jg}^{ln} against time (actually chord lengths traveled) for

$l=0$
$j=0,1,2$
$n=0,1,2,3,4,5$
$g=0,1,2,3,4,5$
$M=1.1,\ 1.2$
$A=4$

TABLE I.—VALUES OF GENERALIZED INDICIAL FORCES, F_{jg}^{ln}

(a) $l=0$; $j=0$; $M=1.1$

$\frac{U_0t'}{c}$	g \ n	0	1	2	3	4	5	g \ n	0	1	2	3	4	5	g \ n	0	1	2	3	4	5
0	0	3.636	3.636	4.848	7.273	11.64	19.39	1	3.636	4.848	7.273	11.64	19.39	33.25	2	4.848	7.273	11.64	19.39	33.25	58.18
.055		3.592	3.637	4.853	7.286	11.67	19.48		3.636	4.848	7.277	11.65	19.45	33.39		4.848	7.273	11.64	19.42	33.33	58.41
.11		3.550	3.637	4.865	7.323	11.77	19.73		3.633	4.848	7.289	11.70	19.59	33.78		4.848	7.273	11.66	19.49	33.57	59.07
.22		3.475	3.640	4.908	7.456	12.13	20.62		3.625	4.849	7.334	11.88	20.13	35.21		4.847	7.273	11.72	19.76	34.42	61.15
.33		3.409	3.644	4.968	7.645	12.64	21.91		3.613	4.849	7.396	12.13	20.89	37.26		4.845	7.273	11.80	20.14	35.64	64.87
.44		3.353	3.649	5.037	7.863	13.23	23.44		3.599	4.850	7.469	12.42	21.78	39.69		4.840	7.273	11.90	20.57	37.05	68.90
.524		3.317	3.652	5.089	8.031	13.70	24.66		3.589	4.851	7.525	12.65	22.47	41.62		4.836	7.273	11.97	20.91	38.16	72.10
.579		3.319	3.679	5.174	8.251	14.24	26.00		3.602	4.883	7.628	12.95	23.20	43.75		4.864	7.320	12.12	21.38	39.48	75.64
.786		3.420	3.871	5.564	9.105	16.20	30.63		3.753	5.128	8.152	14.18	26.29	51.17		5.052	7.685	12.92	23.32	44.38	88.05
1.0		3.562	4.195	6.023	10.10	18.48	36.09		3.942	5.429	8.774	15.62	29.78	59.85		5.370	8.132	13.87	25.59	50.05	102.6
1.571		3.934	4.719	7.259	12.86	25.11	52.66		4.421	6.217	10.45	19.60	39.79	85.93		6.077	9.301	16.43	31.87	66.29	145.8
2.2		4.286	5.325	8.551	15.92	32.86	73.29		4.872	6.962	12.18	23.95	51.36	117.9		6.738	10.45	19.07	38.68	84.89	198.4
2.75		4.547	5.778	9.676	18.54	39.81	92.65		5.203	7.694	13.59	27.63	61.60	147.6		7.225	11.34	21.20	44.43	101.3	240.9
3.667		4.910	6.488	11.21	22.68	51.27	126.0		5.659	8.470	15.73	33.42	78.34	198.1		7.895	12.63	24.44	53.42	127.9	320.2
5.5		5.457	7.581	13.85	29.79	71.74	188.0		6.338	9.856	19.23	43.28	108.0	291.4		8.882	14.67	29.72	68.68	174.9	480.0
7.333		5.860	8.372	16.75	34.88	86.41	232.6		6.834	10.86	21.75	50.35	129.2	358.2		9.602	16.15	33.52	79.62	208.6	588.1
11.0		6.348	9.162	17.38	38.74	96.43	260.3		7.430	11.87	23.96	55.84	144.1	400.7		10.46	17.65	36.90	88.24	232.4	657.7
0	3	7.273	11.64	19.39	33.25	58.18	103.4	4	11.64	19.39	33.25	58.18	103.4	186.2	5	19.39	33.25	58.18	103.4	186.2	338.5
.055		7.273	11.64	19.40	33.29	58.32	103.8		11.64	19.39	33.26	58.25	103.7	186.9		19.39	33.25	58.20	103.6	186.6	339.8
.11		7.273	11.64	19.43	33.41	58.72	105.0		11.64	19.39	33.30	58.45	104.4	188.9		19.39	33.25	58.27	103.9	187.8	343.3
.22		7.273	11.64	19.52	33.83	60.14	109.0		11.64	19.39	33.44	59.16	106.8	196.0		19.39	33.25	58.51	105.1	192.0	355.9
.33		7.272	11.64	19.64	34.44	62.16	114.9		11.64	19.39	33.64	60.16	110.3	206.2		19.39	33.25	58.82	106.8	198.1	374.1
.44		7.271	11.64	19.79	35.13	64.52	121.8		11.64	19.39	33.88	61.33	114.3	218.2		19.39	33.25	59.23	108.8	205.2	395.5
.524		7.269	11.64	19.90	35.68	66.37	127.2		11.64	19.39	34.06	62.23	117.5	227.8		19.39	33.25	59.53	110.4	210.7	412.4
.579		7.314	11.71	20.14	37.53	68.58	133.3		11.71	19.52	34.45	63.52	121.3	238.5		19.52	33.46	60.21	112.6	217.4	431.4
.786		7.671	12.29	21.43	39.66	76.86	154.7		12.29	20.49	36.63	69.02	135.6	276.0		20.49	35.12	63.09	122.2	242.8	498.3
1.0		8.104	13.01	22.98	43.43	86.46	179.0		12.99	21.68	39.25	75.47	152.0	319.8		21.67	37.16	68.51	133.5	272.2	576.4
1.571		9.213	14.87	27.13	53.82	113.8	253.7		14.81	24.78	46.25	93.23	199.7	449.5		24.73	42.47	80.63	164.5	355.8	807.3
2.2		10.26	16.70	31.41	65.06	146.1	343.4		16.53	27.81	53.44	112.4	253.6	605.8		27.64	47.67	93.05	198.0	450.7	1085.
2.75		11.03	18.11	34.86	74.52	172.5	425.7		17.81	30.16	59.25	128.5	300.7	749.0		29.83	51.68	103.1	226.0	533.6	1338.
3.667		12.09	20.10	40.07	89.28	216.9	564.7		19.56	33.56	67.98	153.6	377.1	990.2		32.83	57.49	118.1	269.6	667.5	1765.
5.5		13.04	23.39	48.57	114.3	295.0	818.9		22.12	38.92	82.24	195.9	511.0	1430.		37.17	66.65	142.7	343.2	901.9	2541.
7.333		14.77	25.74	54.70	132.2	351.0	1001.		23.98	42.81	92.51	226.3	606.9	1746.		40.34	73.30	160.4	386.0	1070.	3097.
11.0		16.10	28.13	99.18	146.4	390.9	1119.		26.16	46.78	101.7	250.6	672.8	1951.		44.02	80.19	176.3	433.4	1191.	3462.

TABLE I.—VALUES OF GENERALIZED INDICIAL FORCES, F_{ij}^{lm}—Continued

(b) $l=0$; $j=1$; $M=1.1$

$\frac{U_0 t'}{c}$	g \ n	0	1	2	3	4	5	g \ n	0	1	2	3	4	5	g \ n	0	1	2	3	4	5
0	0	1.818	1.818	2.424	3.636	5.818	9.697	1	1.818	2.424	3.636	5.818	9.697	16.62	2	2.424	3.636	5.818	9.697	16.62	29.09
.055		1.793	1.816	2.423	3.639	5.829	9.730		1.815	2.421	3.634	5.820	9.712	16.63		2.421	3.632	5.814	9.698	16.65	29.18
.11		1.764	1.810	2.421	3.645	5.861	9.829		1.807	2.412	3.627	5.825	9.757	16.83		2.412	3.618	5.801	9.703	16.71	29.43
.22		1.694	1.784	2.410	3.668	5.982	10.21		1.775	2.376	3.598	5.841	9.922	17.41		2.375	3.564	5.748	9.712	16.96	30.38
.33		1.609	1.741	2.387	3.695	6.154	10.77		1.723	2.316	3.547	5.853	10.15	18.28		2.313	3.473	5.655	9.705	17.30	31.78
.44		1.512	1.680	2.346	3.709	6.334	11.41		1.650	2.231	3.466	5.836	10.39	19.26		2.225	3.346	5.514	9.647	17.63	33.36
.524		1.432	1.622	2.298	3.695	6.440	11.87		1.583	2.151	3.380	5.786	10.51	19.94		2.141	3.224	5.368	9.539	17.79	34.43
.579		1.399	1.603	2.304	3.762	6.671	12.53		1.555	2.124	3.374	5.863	10.84	20.97		2.111	3.183	5.348	9.643	18.30	36.12
.786		1.367	1.620	2.412	4.096	7.590	14.96		1.546	2.140	3.497	6.311	12.20	24.78		2.115	3.205	5.520	10.32	20.46	42.41
1.0		1.378	1.682	2.587	4.555	8.780	18.04		1.579	2.215	3.719	6.950	13.97	29.62		2.175	3.315	5.848	11.31	23.31	50.41
1.571		1.460	1.902	3.149	6.000	12.56	28.15		1.713	2.489	4.448	8.967	19.59	45.31		2.392	3.717	6.937	14.43	32.31	76.24
2.2		1.568	2.162	3.815	7.764	17.38	41.66		1.867	2.814	5.317	11.42	26.65	66.03		2.635	4.195	8.238	18.22	43.58	110.1
2.75		1.662	2.389	4.406	9.375	21.94	55.00		1.995	3.098	6.089	13.64	33.29	86.27		2.833	4.610	9.393	21.66	54.12	143.0
3.667		1.813	2.755	5.378	12.10	29.90	79.12		2.194	3.557	7.359	17.39	44.79	122.5		3.134	5.282	11.29	27.44	72.30	201.7
5.5		2.096	3.430	7.173	17.22	45.32	127.4		2.552	4.404	9.707	24.43	66.91	194.6		3.661	6.523	14.81	38.26	107.2	317.7
7.333		2.363	4.006	8.635	21.28	57.25	164.1		2.885	5.132	11.63	30.02	84.11	249.6		4.148	7.592	17.70	46.88	134.4	400.6
11.0		2.777	4.689	10.07	24.73	66.38	189.9		3.390	6.008	13.57	34.92	97.58	288.9		4.874	8.890	20.66	54.56	155.9	470.8
0	3	3.636	5.818	9.697	16.62	29.09	51.72	4	5.818	9.697	16.62	29.09	51.72	93.09	5	9.697	16.62	29.09	51.72	93.09	169.3
.055		3.632	5.811	9.689	16.62	29.13	51.86		5.811	9.685	16.61	29.09	51.78	93.34		9.685	16.60	29.07	51.71	93.19	169.7
.11		3.618	5.789	9.667	16.63	29.23	52.28		5.789	9.649	16.57	29.09	51.95	94.07		9.649	16.54	28.99	51.71	93.49	171.0
.22		3.564	5.702	9.573	16.63	29.63	53.88		5.702	9.503	16.40	29.07	52.60	96.83		9.503	16.29	28.70	51.64	94.58	175.8
.33		3.472	5.556	9.409	16.59	30.16	56.24		5.556	9.261	16.11	28.97	53.47	100.9		9.261	15.88	28.18	51.42	96.04	182.0
.44		3.344	5.353	9.163	16.45	30.66	58.87		5.352	8.921	15.68	28.70	54.26	105.4		8.921	15.20	27.41	50.90	97.33	190.8
.524		3.222	5.159	8.911	16.34	30.87	60.63		5.158	8.598	15.24	28.30	54.55	108.4		8.597	14.74	26.63	50.16	97.74	195.9
.579		3.179	5.092	8.872	16.40	31.70	63.50		5.090	8.486	15.16	28.54	55.96	113.3		8.486	14.55	26.49	50.55	100.2	204.7
.786		3.194	5.126	9.135	17.49	35.31	74.22		5.121	8.543	15.59	30.37	62.13	132.0		8.540	14.64	27.21	53.69	111.0	237.9
1.0		3.295	5.302	9.638	19.10	40.07	87.83		5.290	8.835	16.46	33.10	70.34	155.9		8.828	15.15	28.70	58.42	125.4	280.2
1.571		3.652	5.940	11.40	24.22	55.13	131.9		5.890	9.894	19.38	41.78	96.25	232.6		9.852	16.96	33.71	73.51	170.9	416.3
2.2		4.051	6.696	13.49	30.43	73.92	189.3		6.564	11.15	22.86	52.30	128.5	332.4		11.02	19.10	39.70	91.77	227.5	592.0
2.75		4.376	7.353	15.34	36.05	91.46	244.9		7.114	12.24	25.96	61.82	158.6	428.8		11.97	20.96	45.02	108.3	280.2	763.3
3.667		4.884	8.415	18.38	45.47	121.7	343.8		7.936	14.00	31.04	77.76	210.3	600.0		13.39	23.96	53.76	135.9	370.7	1065.
5.5		5.701	10.33	24.02	63.12	179.5	538.9		9.325	17.25	40.47	107.6	309.2	937.0		15.75	29.51	69.96	187.7	543.6	1659.
7.333		6.471	12.07	28.67	77.21	224.6	688.4		10.60	20.05	48.24	131.5	386.4	1196.		17.95	34.29	83.34	229.1	678.8	2115.
11.0		7.601	14.13	33.47	89.87	260.7	797.2		12.45	23.48	56.32	153.0	448.6	1385.		21.06	40.17	97.31	266.7	788.1	2450.

TABLE I.—VALUES OF GENERALIZED INDICIAL FORCES, F_{ij}^{lm}—Continued

(c) $l=0$; $j=2$; $M=1.1$

$\frac{U_0 t'}{c}$	g \ n	0	1	2	3	4	5	g \ n	0	1	2	3	4	5	g \ n	0	1	2	3	4	5
0	0	1.212	1.212	1.616	2.424	3.879	6.465	1	1.212	1.616	2.424	3.879	6.465	11.08	2	1.616	2.424	3.879	6.465	11.08	19.39
.055		1.197	1.212	1.618	2.429	3.891	6.494		1.212	1.616	2.426	3.884	6.482	11.13		1.616	2.424	3.880	6.473	11.11	19.47
.11		1.181	1.211	1.620	2.440	3.923	6.579		1.210	1.614	2.428	3.899	6.531	11.26		1.616	2.422	3.883	6.494	11.19	19.70
.22		1.141	1.203	1.625	2.475	4.037	6.890		1.197	1.602	2.427	3.940	6.696	11.76		1.601	2.403	3.877	6.551	11.45	20.51
.33		1.088	1.179	1.619	2.509	4.184	7.333		1.166	1.563	2.404	3.972	6.902	12.44		1.567	2.353	3.838	6.585	11.76	21.63
.44		1.015	1.132	1.589	2.514	4.310	7.788		1.111	1.503	2.340	3.953	7.061	13.15		1.499	2.254	3.721	6.530	11.98	22.76
.524		.9418	1.075	1.531	2.476	4.342	8.058		1.047	1.425	2.249	3.870	7.073	13.52		1.418	2.136	3.569	6.375	11.99	23.32
.579		.9099	1.052	1.531	2.506	4.482	8.496		1.018	1.393	2.226	3.897	7.267	14.19		1.394	2.088	3.526	6.402	12.20	24.41
.786		.8653	1.041	1.570	2.703	5.080	10.16		.9873	1.373	2.268	4.149	8.135	16.78		1.355	2.056	3.574	6.770	13.02	28.00
1.0		.8553	1.066	1.670	2.988	5.888	12.32		.9910	1.401	2.389	4.549	9.326	20.15		1.371	2.096	3.749	7.381	15.52	34.22
1.571		.8745	1.179	2.017	3.963	8.534	19.60		1.041	1.539	2.828	5.877	13.21	31.39		1.465	2.296	4.389	9.421	21.72	52.04
2.2		.9157	1.326	2.435	5.141	11.89	29.35		1.112	1.719	3.366	7.495	18.10	46.26		1.531	2.559	5.194	11.91	29.47	70.70
2.75		.9559	1.460	2.840	6.319	15.35	39.70		1.170	1.884	3.884	9.104	23.09	61.86		1.679	2.798	5.961	14.38	37.36	102.1
3.667		1.027	1.686	3.507	8.299	21.36	58.42		1.267	2.164	4.745	11.80	31.71	89.85		1.832	3.205	7.239	18.51	50.93	147.3
5.5		1.183	2.139	4.816	12.22	33.55	97.51		1.467	2.727	6.439	17.14	49.08	147.9		2.130	4.027	9.764	26.63	78.23	240.5
7.333		1.372	2.578	5.962	15.40	42.79	125.2		1.712	3.278	7.941	21.53	62.44	189.6		2.498	4.833	12.02	33.45	99.30	308.1
11.0		1.719	3.169	7.249	18.65	51.84	152.4		2.130	4.037	9.672	26.08	75.96	230.5		3.092	5.957	14.65	40.55	120.4	374.4
0	3	2.424	3.879	6.465	11.08	19.39	34.48	4	3.879	6.465	11.08	19.39	34.48	62.06	5	6.465	11.08	19.39	34.48	62.00	112.8
.055		2.424	3.878	6.467	11.10	19.44	34.61		3.878	6.464	11.09	19.42	34.56	62.30		6.464	11.08	19.40	34.52	62.20	113.3
.11		2.422	3.875	6.470	11.13	19.57	35.00		3.875	6.458	11.09	19.47	34.77	62.96		6.458	11.07	19.41	34.61	62.58	114.4
.22		2.403	3.845	6.456	11.21	19.99	36.37		3.845	6.408	11.06	19.61	35.49	65.36		6.408	10.98	19.35	34.83	63.82	118.7
.33		2.352	3.764	6.377	11.25	20.49	38.28		3.764	6.273	10.92	19.65	36.32	68.65		6.273	10.75	19.10	34.88	65.41	124.4
.44		2.253	3.606	6.183	11.13	20.83	40.15		3.605	6.010	10.58	19.42	36.84	71.86		6.009	10.30	18.49	34.43	66.08	130.1
.524		2.134	3.418	5.923	10.85	20.75	41.04		3.417	5.697	10.13	18.90	36.65	73.31		5.696	9.765	17.69	33.48	65.64	132.5
.579		2.085	3.340	5.845	10.88	21.21	42.88		3.339	5.567	9.988	18.93	37.42	76.49		5.566	9.543	17.44	33.51	66.90	138.1
.786		2.048	3.289	5.910	11.46	23.47	50.09		3.285	5.481	10.08	19.88	41.26	89.01		5.479	9.395	17.59	35.13	73.65	160.2
1.0		2.081	3.352	6.183	12.45	26.63	59.56		3.343	5.585	10.53	21.54	46.69	105.5		5.579	9.574	18.35	38.00	83.16	189.5
1.571		2.245	3.668	7.208	15.77	36.96	90.85		3.628	6.109	12.23	27.16	64.42	160.0		6.075	10.47	21.26	47.71	114.2	285.9
2.2		2.445	4.082	8.493	19.83	49.84	131.7		3.974	6.794	14.36	34.03	86.49	230.8		6.663	11.64	24.90	59.60	152.9	411.1
2.75		2.611	4.459	9.703	23.84	62.94	174.4		4.263	7.418	16.38	40.78	108.9	304.8		7.192	12.70	28.38	71.31	192.1	541.7
3.667		2.866	5.100	11.75	30.56	85.41	250.3		4.702	8.477	19.78	52.13	147.3	436.0		7.964	14.51	34.20	90.94	259.2	772.8
5.5		3.343	6.396	15.77	43.85	130.5	406.7		5.500	10.62	26.50	74.55	224.3	705.7		9.322	18.16	45.73	129.8	393.7	1248.
7.333		3.943	7.670	19.39	54.90	165.6	520.8		6.522	12.72	32.54	93.25	284.5	903.2		11.14	21.76	56.10	162.2	499.0	1590.
11.0		4.853	9.458	23.65	66.58	200.6	632.5		7.982	15.70	39.72	113.1	344.6	1097.		13.55	26.84	68.51	196.8	604.4	1938.

TABLE I.—VALUES OF GENERALIZED INDICIAL FORCES, F^*_{ij}—Continued

(d) $l=1$; $j=1$; $M=1.1$

$\frac{Ut'}{c}$	g \ n	0	1	2	3	4	5	g \ n	0	1	2	3	4	5	g \ n	0	1	2	3	4	5
0	0	1.212	1.212	1.616	2.424	3.879	6.465	1	1.212	1.616	2.424	3.879	6.465	11.08	2	1.616	2.424	3.879	6.465	11.08	19.39
.055		1.108	1.212	1.618	2.429	3.890	6.493		1.212	1.616	2.426	3.885	6.482	11.13		1.616	2.424	3.881	6.474	11.11	19.47
.11		1.185	1.213	1.622	2.442	3.924	6.575		1.212	1.617	2.431	3.902	6.532	11.26		1.616	2.426	3.888	6.500	11.19	19.60
.22		1.107	1.219	1.641	2.490	4.044	6.866		1.214	1.623	2.453	3.970	6.716	11.73		1.623	2.435	3.921	6.604	11.49	20.47
.33		1.160	1.232	1.675	2.568	4.226	7.290		1.223	1.640	2.496	4.080	6.994	12.41		1.639	2.460	3.982	6.776	11.94	21.62
.44		1.169	1.258	1.724	2.675	4.461	7.821		1.245	1.673	2.564	4.235	7.353	13.27		1.671	2.510	4.089	7.022	12.54	23.07
.524		1.188	1.289	1.779	2.779	4.681	8.302		1.271	1.713	2.638	4.390	7.700	14.05		1.709	2.568	4.203	7.270	13.10	24.39
.579		1.204	1.313	1.821	2.873	4.881	8.751		1.292	1.745	2.701	4.527	8.013	14.78		1.740	2.616	4.299	7.488	13.61	25.61
.786		1.278	1.415	1.997	3.201	5.562	10.24		1.383	1.878	2.942	5.017	9.080	17.20		1.869	2.815	4.674	8.276	15.38	29.70
1.0		1.353	1.520	2.176	3.549	6.299	11.88		1.475	2.014	3.193	5.534	10.23	19.85		1.999	3.018	5.063	9.106	17.27	34.17
1.571		1.530	1.770	2.621	4.451	8.287	16.53		1.691	2.339	3.810	6.861	13.29	27.27		2.306	3.503	6.021	11.23	22.29	46.59
2.2		1.635	2.000	3.068	5.391	10.49	21.97		1.880	2.636	4.409	8.225	16.63	35.83		2.578	3.945	6.939	13.39	27.71	60.82
2.75		1.796	2.169	3.383	6.111	12.23	26.48		2.017	2.855	4.855	9.264	19.25	42.86		2.773	4.270	7.625	15.03	31.96	72.41
3.667		1.942	2.401	3.852	7.193	14.95	33.77		2.196	3.153	5.492	10.81	23.32	54.14		3.013	4.712	8.599	17.46	38.51	90.95
5.5		2.137	2.721	4.519	8.784	19.09	45.27		2.435	3.564	6.395	13.07	29.45	71.75		3.376	5.321	9.977	21.00	48.34	119.8
7.333		2.244	2.897	4.896	9.738	21.81	53.68		2.561	3.791	6.905	14.41	33.39	84.30		3.552	5.657	10.75	23.09	54.60	140.0
11.0		2.314	2.990	5.068	10.05	22.29	53.94		2.660	3.919	7.144	14.88	34.05	85.11		3.633	5.847	11.12	23.84	56.01	141.7
0	3	2.424	3.879	6.465	11.08	19.39	34.48	4	3.879	6.465	11.08	19.39	34.48	62.06	5	6.464	11.08	19.39	34.48	62.06	112.8
.055		2.424	3.879	6.468	11.10	19.44	34.61		3.879	6.465	11.09	19.42	34.56	62.29		6.465	11.08	19.40	34.52	62.20	113.2
.11		2.426	3.881	6.479	11.14	19.57	34.98		3.881	6.468	11.11	19.49	34.79	62.95		6.468	11.09	19.43	34.64	62.61	114.4
.22		2.435	3.896	6.530	11.31	20.07	36.33		3.896	6.493	11.19	19.78	35.65	65.31		6.493	11.13	19.53	35.14	64.11	118.6
.33		2.460	3.936	6.632	11.59	20.83	38.31		3.936	6.561	11.36	20.26	36.97	68.78		6.561	11.25	19.86	35.97	66.35	124.8
.44		2.509	4.015	6.802	12.00	21.95	40.81		4.015	6.692	11.65	20.96	38.73	73.20		6.692	11.47	20.37	37.20	69.55	132.7
.524		2.567	4.109	6.989	12.41	22.81	43.10		4.109	6.849	11.97	21.67	40.41	77.24		6.849	11.74	20.92	38.45	72.53	140.0
.579		2.615	4.186	7.147	12.78	23.68	45.22		4.185	6.976	12.23	22.29	41.93	80.98		6.976	11.96	21.38	39.54	75.23	146.7
.786		2.811	4.503	7.762	14.10	26.69	52.30		4.501	7.504	13.28	24.57	47.18	93.43		7.504	12.86	23.20	43.55	84.56	166.0
1.0		3.012	4.828	8.399	15.49	29.91	60.03		4.825	8.046	14.36	26.96	52.68	107.1		8.044	13.79	25.08	47.76	94.52	193.5
1.571		3.484	5.602	9.963	19.02	38.44	81.44		5.589	9.335	17.01	33.04	67.63	144.8		9.326	16.00	29.63	58.42	120.8	260.7
2.2		3.906	6.307	11.46	22.62	47.61	105.9		6.276	10.51	19.54	39.13	83.54	187.5		10.48	18.01	34.08	69.19	143.9	336.8
2.75		4.209	6.825	12.58	25.34	54.77	125.6		6.771	11.37	21.43	43.85	95.92	222.1		11.32	19.49	37.35	77.34	170.7	398.3
3.667		4.612	7.529	14.16	29.36	65.76	157.2		7.431	12.54	24.10	50.72	114.9	277.1		12.43	21.49	41.96	89.34	204.2	495.9
5.5		5.160	8.498	16.40	35.21	82.24	206.1		8.312	14.15	27.87	60.69	143.3	362.3		13.92	24.25	48.47	106.7	254.1	646.7
7.333		5.415	9.034	17.66	38.64	92.66	240.2		8.730	15.04	20.99	66.54	161.2	421.2		14.60	25.77	52.14	116.9	285.5	750.7
11.0		5.620	9.335	18.26	39.91	95.12	243.4		9.089	15.54	31.01	68.73	164.1	427.2		15.24	26.63	53.92	120.8	293.3	761.9

TABLE I.—VALUES OF GENERALIZED INDICIAL FORCES, F^*_{ij}—Continued

(e) $l=0$; $j=0$; $M=1.2$

$\frac{Ut'}{c}$	g \ n	0	1	2	3	4	5	g \ n	0	1	2	3	4	5	g \ n	0	1	2	3	4	5
0	0	3.333	3.333	4.444	6.667	10.67	17.78	1	3.333	4.444	6.667	10.67	17.78	30.48	2	4.444	6.667	10.67	17.78	30.48	53.33
.06		3.293	3.334	4.448	6.679	10.70	17.86		3.333	4.444	6.671	10.68	17.83	30.60		4.444	6.667	10.67	17.80	30.55	53.55
.12		3.255	3.334	4.460	6.713	10.79	18.09		3.330	4.444	6.682	10.73	17.96	30.97		4.444	6.667	10.69	17.87	30.77	54.15
.24		3.187	3.337	4.499	6.835	11.12	18.91		3.323	4.445	6.723	10.89	18.45	32.28		4.443	6.667	10.74	18.11	31.55	56.34
.36		3.128	3.340	4.556	7.009	11.59	20.09		3.312	4.445	6.781	11.12	19.15	34.17		4.441	6.667	10.82	18.46	32.67	59.49
.48		3.080	3.345	4.619	7.211	12.14	21.50		3.299	4.446	6.847	11.39	19.97	36.41		4.437	6.667	10.91	18.87	33.93	63.20
.545		3.058	3.347	4.654	7.325	12.45	22.31		3.292	4.446	6.885	11.54	20.44	37.69		4.435	6.667	10.96	19.09	34.72	65.32
.6		3.061	3.369	4.710	7.460	12.77	23.10		3.307	4.474	6.956	11.73	20.93	38.94		4.459	6.707	11.06	19.39	35.52	67.42
.8		3.147	3.521	5.013	8.107	14.23	26.49		3.432	4.672	7.366	12.67	23.17	44.39		4.046	7.002	11.69	20.87	39.18	76.54
1.0		3.262	3.706	5.355	8.821	15.83	30.22		3.583	4.907	7.834	13.72	25.63	50.36		4.867	7.352	12.41	22.53	43.20	86.54
1.5		3.552	4.163	6.202	10.62	19.94	40.08		3.952	5.484	8.993	16.33	31.92	66.04		5.401	8.211	14.19	26.68	53.46	112.7
2.0		3.808	4.551	6.975	12.31	23.94	50.01		4.274	5.997	10.05	18.78	37.97	81.67		5.867	8.974	15.81	30.55	63.29	138.7
2.4		3.988	4.833	7.531	13.55	26.92	57.60		4.498	6.360	10.81	20.56	42.48	93.56		6.192	9.513	16.97	33.37	70.58	158.3
3.0		4.221	5.200	8.260	15.19	30.91	67.85		4.788	6.833	11.80	22.92	48.48	109.6		6.612	10.21	18.49	37.08	80.29	184.8
4.0		4.533	5.681	9.196	17.28	35.95	80.75		5.172	7.453	13.08	25.93	56.07	129.7		7.162	11.13	20.46	41.83	92.59	218.1
6.0		4.894	6.173	10.06	18.99	39.72	89.60		5.602	8.094	14.28	28.46	61.87	143.8		7.771	12.09	22.31	45.88	102.1	241.7
0	3	6.667	10.67	17.78	30.48	53.33	94.81	4	10.67	17.78	30.48	53.33	94.81	170.7	5	17.78	30.48	53.33	94.81	170.7	310.3
.06		6.667	10.67	17.79	30.51	53.46	95.18		10.67	17.78	30.49	53.40	95.03	171.3		17.78	30.48	53.35	94.92	171.1	311.4
.12		6.667	10.67	17.81	30.62	53.83	96.22		10.67	17.78	30.53	53.58	95.66	173.1		17.78	30.48	53.42	95.24	172.1	314.7
.24		6.667	10.67	17.89	31.01	55.13	99.96		10.67	17.78	30.66	54.23	97.89	179.7		17.78	30.48	53.63	96.35	176.1	326.3
.36		6.666	10.67	18.01	31.57	57.00	105.4		10.67	17.78	30.84	55.16	101.1	189.1		17.78	30.48	53.94	97.94	181.6	343.1
.48		6.665	10.67	18.14	32.22	59.18	111.7		10.67	17.78	31.06	56.23	104.8	200.2		17.78	30.48	54.30	99.79	188.2	362.8
.545		6.664	10.67	18.22	32.58	60.41	115.3		10.67	17.78	31.18	56.84	106.9	206.5		17.78	30.48	54.60	100.8	191.9	374.0
.6		6.703	10.73	18.39	33.06	61.75	118.9		10.73	17.89	31.46	57.66	109.3	212.9		17.88	30.66	54.99	102.3	196.0	385.3
.8		6.903	11.20	19.40	35.53	67.95	134.7		11.20	18.67	33.18	61.89	120.0	240.5		18.67	32.01	57.97	109.7	215.0	434.7
1.0		7.335	11.76	20.58	38.29	74.77	151.9		11.75	19.60	35.16	66.62	131.9	270.8		19.60	33.60	61.41	117.9	236.0	488.8
1.5		8.165	13.13	23.48	45.19	92.12	196.9		13.10	21.88	40.07	78.44	162.0	349.8		21.86	37.51	69.91	138.6	289.2	629.6
2.0		8.892	14.35	26.11	51.61	108.7	241.4		14.29	23.91	44.52	89.43	190.8	427.7		23.86	40.98	77.61	157.9	340.0	768.3
2.4		9.390	15.21	28.00	56.28	121.0	275.0		15.12	25.34	47.70	97.42	212.1	486.5		25.26	43.43	83.13	171.8	377.5	872.9
3.0		10.05	16.32	30.47	62.43	137.4	320.2		16.19	27.20	51.87	107.9	240.3	565.6		27.07	46.61	90.34	190.2	427.4	1013.
4.0		10.92	17.79	33.67	70.31	158.1	377.2		17.60	29.63	57.27	121.4	276.2	665.1		29.45	50.79	99.70	213.8	490.7	1190.
6.0		11.85	19.32	36.71	77.07	174.3	417.8		19.10	32.18	62.43	133.0	304.3	736.5		31.97	55.15	108.7	234.2	540.5	1318.

TABLE I.—VALUES OF GENERALIZED INDICIAL FORCES, F_{ij}^{kl}—Continued

(f) $l=0$; $j=1$; $M=1.2$

$\frac{Vt'}{c}$	g \ n	0	1	2	3	4	5	g \ n	0	1	2	3	4	5	g \ n	0	1	2	3	4	5
0	0	1.667	1.667	2.222	3.333	5.333	8.889	1	1.667	2.222	3.333	5.333	8.889	15.24	2	2.222	3.333	5.333	8.889	15.24	26.67
.06		1.644	1.665	2.222	3.335	5.343	8.919		1.664	2.219	3.331	5.335	8.902	15.28		2.219	3.329	5.329	8.890	15.26	26.74
.12		1.617	1.659	2.219	3.342	5.373	9.010		1.657	2.211	3.325	5.340	8.944	15.43		2.211	3.317	5.318	8.894	15.32	26.98
.24		1.553	1.635	2.209	3.363	5.484	9.357		1.627	2.178	3.299	5.355	9.097	15.97		2.177	3.267	5.270	8.904	15.55	27.85
.36		1.476	1.596	2.189	3.389	5.645	9.881		1.579	2.123	3.252	5.387	9.315	16.77		2.120	3.183	5.185	8.900	15.87	29.16
.48		1.388	1.540	2.153	3.405	5.821	10.50		1.512	2.045	3.179	5.357	9.542	17.71		2.040	3.067	5.057	8.863	16.20	30.67
.545		1.337	1.503	2.124	3.403	5.904	10.83		1.469	1.994	3.126	5.333	9.643	18.21		1.987	2.989	4.966	8.797	16.33	31.46
.6		1.312	1.489	2.123	3.434	6.026	11.19		1.450	1.974	3.116	5.366	9.816	18.78		1.964	2.959	4.944	8.838	16.60	32.39
.8		1.294	1.510	2.214	3.699	6.732	13.02		1.451	1.997	3.224	5.727	10.87	21.65		1.978	2.992	5.099	9.387	18.28	37.15
1.0		1.313	1.568	2.357	4.049	7.600	15.20		1.489	2.069	3.409	6.219	12.17	25.09		2.041	3.098	5.375	10.15	20.39	42.86
1.5		1.405	1.756	2.778	5.048	10.07	21.46		1.623	2.307	3.967	7.367	15.88	34.93		2.248	3.450	6.217	12.37	26.38	59.10
2.0		1.514	1.958	3.220	6.068	12.68	28.28		1.771	2.564	4.557	9.128	19.81	45.58		2.469	3.831	7.110	14.70	32.71	76.74
2.4		1.604	2.119	3.568	6.925	14.78	33.79		1.888	2.769	5.022	10.30	22.93	54.15		2.644	4.134	7.818	16.54	37.74	90.80
3.0		1.737	2.350	4.062	8.095	17.74	41.64		2.059	3.065	5.686	11.96	27.35	66.32		2.896	4.571	8.627	19.15	44.84	110.9
4.0		1.949	2.697	4.773	9.731	21.80	52.24		2.325	3.509	6.647	14.30	33.43	82.82		3.284	5.230	10.29	22.82	54.05	138.1
6.0		2.258	3.122	5.518	11.24	25.14	60.14		2.694	4.063	7.688	16.52	38.55	93.38		3.805	6.056	11.91	26.37	63.05	160.1
0	3	3.333	5.333	8.889	15.24	26.67	47.41	4	5.333	8.889	15.24	26.67	47.41	85.33	5	8.889	15.24	26.67	47.41	85.33	155.2
.06		3.329	5.327	8.882	15.24	26.70	47.54		5.327	8.878	15.23	26.67	47.46	85.56		8.878	15.22	26.64	47.40	85.42	155.5
.12		3.317	5.307	8.861	15.24	26.80	47.93		5.307	8.845	15.19	26.67	47.63	86.23		8.845	15.16	26.58	47.40	85.70	156.7
.24		3.267	5.227	8.775	15.24	27.16	49.41		5.227	8.711	15.04	26.65	48.22	88.78		8.711	14.93	26.30	47.34	86.71	161.2
.36		3.183	5.093	8.626	15.21	27.67	51.61		5.093	8.489	14.77	26.56	49.04	92.57		8.489	14.55	25.83	47.15	88.09	167.8
.48		3.065	4.907	8.403	15.10	28.16	54.12		4.906	8.178	14.38	26.34	49.83	96.88		8.178	14.02	25.13	46.70	89.39	175.4
.545		2.987	4.782	8.246	14.99	28.36	55.42		4.782	7.971	14.10	26.11	50.13	99.09		7.970	13.66	24.65	46.29	89.84	179.2
.6		2.956	4.734	8.205	15.04	28.79	56.99		4.733	7.889	14.03	26.20	50.85	101.8		7.889	13.52	24.51	46.42	91.07	181.0
.8		2.985	4.786	8.446	15.93	31.59	65.12		4.783	7.976	14.43	27.69	55.66	116.0		7.974	13.67	25.18	48.99	99.51	209.2
1.0		3.085	4.955	8.889	17.19	35.13	74.91		4.948	8.257	15.17	29.83	61.77	133.1		8.253	14.15	26.46	52.71	110.3	239.7
1.5		3.415	5.515	10.25	20.84	45.20	102.8		5.492	9.189	17.45	36.05	79.16	181.9		9.172	15.75	30.39	63.55	140.9	320.4
2.0		3.767	6.122	11.69	24.69	55.84	132.8		6.064	10.20	19.88	42.61	97.54	234.3		10.16	17.48	34.59	74.98	173.3	419.5
2.4		4.044	6.603	12.84	27.72	64.28	156.9		6.530	11.00	21.80	47.77	112.1	276.3		10.93	18.85	37.91	83.99	198.9	494.0
3.0		4.443	7.299	14.47	32.02	76.20	191.0		7.187	12.16	24.55	55.10	132.7	335.9		12.05	20.83	42.65	96.77	235.1	599.8
4.0		5.052	8.348	16.85	38.10	92.70	237.4		8.186	13.90	28.56	65.48	161.2	417.0		13.74	23.82	49.59	114.9	285.3	743.8
6.0		5.853	9.667	19.49	44.02	107.0	273.5		9.483	16.10	33.04	75.66	186.0	480.4		15.91	27.58	57.37	132.8	329.2	857.0

TABLE I.—VALUES OF GENERALIZED INDICIAL FORCES, F_{ik}^{kl}—Continued

(g) $l=0$; $j=2$; $M=1.2$

$\frac{Vt'}{c}$	g \ n	0	1	2	3	4	5	g \ n	0	1	2	3	4	5	g \ n	0	1	2	3	4	5
0	0	1.111	1.111	1.481	2.222	3.556	5.926	1	1.111	1.481	2.222	3.556	5.926	10.16	2	1.481	2.222	3.556	5.926	10.16	17.78
.06		1.097	1.111	1.483	2.226	3.566	5.953		1.111	1.481	2.223	3.561	5.942	10.20		1.481	2.222	3.557	5.933	10.18	17.85
.12		1.082	1.110	1.485	2.236	3.596	6.030		1.109	1.480	2.225	3.573	5.985	10.32		1.480	2.220	3.559	5.952	10.25	18.05
.24		1.045	1.102	1.489	2.267	3.698	6.312		1.096	1.467	2.223	3.609	6.133	10.77		1.467	2.201	3.551	6.001	10.48	18.70
.36		.9948	1.078	1.480	2.295	3.828	6.712		1.066	1.434	2.198	3.633	6.314	11.39		1.432	2.150	3.504	6.023	10.76	19.80
.48		.9241	1.031	1.445	2.294	3.939	7.136		1.011	1.368	2.132	3.606	6.451	12.03		1.364	2.052	3.390	5.956	10.94	20.82
.545		.8754	.9921	1.409	2.271	3.966	7.326		.9672	1.315	2.071	3.553	6.468	12.30		1.310	1.972	3.288	5.855	10.95	21.24
.6		.8494	.9734	1.397	2.278	4.031	7.555		.9447	1.289	2.047	3.551	6.552	12.65		1.282	1.933	3.245	5.842	11.07	21.79
.8		.8158	.9664	1.435	2.429	4.482	8.792		.9235	1.277	2.082	3.746	7.210	14.58		1.263	1.912	3.287	6.128	12.10	24.97
1.0		.8127	.9902	1.515	2.650	5.067	10.32		.9322	1.304	2.180	4.049	8.080	16.98		1.283	1.953	3.430	6.594	13.50	28.93
1.5		.8447	1.090	1.774	3.316	6.800	14.85		.9914	1.428	2.515	4.980	10.65	24.05		1.382	2.133	3.929	8.035	17.62	40.60
2.0		.9007	1.209	2.065	4.050	8.707	19.97		1.069	1.578	2.896	6.008	13.49	32.00		1.503	2.354	4.500	9.633	22.18	53.67
2.4		.9461	1.310	2.304	4.650	10.28	24.24		1.136	1.706	3.211	6.850	15.82	38.59		1.606	2.543	4.975	10.94	25.91	64.40
3.0		1.027	1.466	2.660	5.533	12.69	30.50		1.243	1.903	3.635	8.093	19.24	48.26		1.768	2.834	5.691	12.88	31.30	80.30
4.0		1.175	1.725	3.221	6.871	15.99	39.54		1.431	2.232	4.434	9.991	24.30	62.28		2.048	3.321	6.829	15.85	39.54	103.4
6.0		1.442	2.096	3.871	8.188	18.92	46.53		1.753	2.716	5.343	11.93	28.81	73.37		2.501	4.042	8.238	18.95	46.91	121.0
0	3	2.222	3.556	5.926	10.16	17.78	31.61	4	3.556	5.926	10.16	17.78	31.61	56.89	5	5.926	10.16	17.78	31.61	56.89	103.4
.06		2.222	3.555	5.928	10.17	17.82	31.73		3.555	5.925	10.16	17.80	31.68	57.10		5.925	10.16	17.78	31.64	57.01	103.8
.12		2.220	3.551	5.930	10.20	17.93	32.08		3.551	5.918	10.16	17.85	31.87	57.71		5.919	10.15	17.79	31.72	57.35	104.9
.24		2.201	3.521	5.913	10.27	18.31	33.32		3.521	5.869	10.13	17.96	32.51	59.88		5.869	10.06	17.72	31.90	58.46	108.7
.36		2.150	3.440	5.830	10.29	18.75	35.03		3.440	5.734	9.984	17.97	33.23	62.83		5.734	9.830	17.46	31.90	59.68	113.9
.48		2.051	3.283	5.632	10.15	19.02	36.72		3.282	5.471	9.637	17.71	33.64	65.71		5.471	9.379	16.84	31.40	60.33	118.9
.545		1.970	3.155	5.457	9.970	18.99	37.39		3.154	5.258	9.332	17.37	33.55	66.82		5.258	9.014	16.31	30.77	60.12	120.8
.6		1.931	3.092	5.383	9.936	19.18	38.32		3.091	5.153	9.201	17.30	33.85	68.40		5.153	8.834	16.07	30.63	60.60	123.0
.8		1.907	3.059	5.440	10.39	20.89	43.72		3.056	5.097	9.287	18.04	36.77	77.80		5.096	8.738	16.21	31.90	65.70	140.2
1.0		1.943	3.123	5.667	11.14	23.22	50.48		3.117	5.204	9.662	19.32	40.77	89.59		5.201	8.921	16.85	34.11	72.71	161.1
1.5		2.106	3.410	6.464	13.50	30.12	70.39		3.391	5.681	10.99	23.32	52.66	124.3		5.667	9.738	19.13	41.06	93.60	222.8
2.0		2.303	3.761	7.382	16.13	37.75	92.64		3.720	6.264	12.53	27.77	65.76	163.1		6.229	10.74	21.78	48.80	116.7	291.0
2.4		2.470	4.060	8.147	18.28	43.99	111.0		3.998	6.761	13.81	31.43	76.55	195.2		6.704	11.59	23.99	55.17	135.6	348.4
3.0		2.728	4.523	9.300	21.47	53.17	138.0		4.428	7.531	15.75	36.35	92.34	242.2		7.437	12.90	27.33	64.60	163.3	431.8
4.0		3.171	5.298	11.14	26.36	66.85	177.3		5.158	8.818	18.84	45.19	115.9	310.8		8.676	15.11	32.67	79.15	204.9	553.4
6.0		3.868	6.449	13.45	31.54	79.35	209.2		6.288	10.73	22.76	54.09	137.7	366.7		10.57	18.39	39.46	94.77	243.4	653.3

TABLE I.—VALUES OF GENERALIZED INDICIAL FORCES, F_{gn}—Concluded
(h) $l=1$; $j=1$; $M=1.2$

$\frac{U_0 t'}{c}$	g \ n	0	1	2	3	4	5	g \ n	0	1	2	3	4	5	g \ n	0	1	2	3	4	5
0	0	1.111	1.111	1.482	2.222	3.556	5.926	1	1.111	1.482	2.222	3.556	5.926	10.16	2	1.482	2.222	3.556	5.926	10.16	17.78
.06		1.098	1.111	1.483	2.226	3.566	5.953		1.111	1.482	2.224	3.561	5.942	10.20		1.482	2.222	3.558	5.934	10.18	17.85
.12		1.087	1.112	1.487	2.238	3.597	6.028		1.111	1.482	2.228	3.577	5.988	10.32		1.482	2.224	3.564	5.959	10.26	18.05
.24		1.071	1.118	1.505	2.284	3.709	6.297		1.113	1.489	2.250	3.641	6.159	10.76		1.488	2.233	3.595	6.056	10.53	18.78
.36		1.067	1.131	1.538	2.357	3.879	6.691		1.123	1.506	2.291	3.745	6.419	11.39		1.505	2.258	3.657	6.220	10.96	19.84
.48		1.078	1.157	1.587	2.458	4.099	7.184		1.144	1.539	2.358	3.893	6.761	12.19		1.537	2.308	3.759	6.455	11.52	21.19
.545		1.091	1.177	1.622	2.527	4.241	7.493		1.163	1.565	2.407	3.995	6.985	12.69		1.563	2.348	3.838	6.619	11.89	22.04
.6		1.106	1.198	1.656	2.591	4.371	7.771		1.181	1.592	2.455	4.091	7.189	13.15		1.588	2.387	3.910	6.773	12.23	22.81
.8		1.165	1.279	1.789	2.839	4.875	8.848		1.254	1.698	2.642	4.463	7.981	14.90		1.691	2.545	4.202	7.373	13.54	25.79
1.0		1.225	1.358	1.920	3.086	5.381	9.949		1.326	1.801	2.827	4.833	8.775	16.69		1.792	2.700	4.490	7.969	14.85	28.81
1.5		1.354	1.532	2.214	3.652	6.571	12.62		1.481	2.028	3.239	5.676	10.63	20.99		2.010	3.039	5.131	9.324	17.92	36.05
2.0		1.454	1.671	2.456	4.132	7.614	15.02		1.603	2.210	3.577	6.385	12.24	24.84		2.182	3.310	5.655	10.46	20.56	42.49
2.4		1.521	1.761	2.614	4.451	8.321	16.68		1.681	2.327	3.798	6.857	13.33	27.49		2.293	3.485	5.998	11 21	22.34	46.92
3.0		1.597	1.807	2.800	4.829	9.161	18.68		1.772	2.465	4.057	7.412	14.62	30.66		2.422	3.690	6.400	12.10	24.45	52.21
4.0		1.679	1.978	2.988	5.205	9.981	20.60		1.870	2.610	4.324	7.968	15.88	33.72		2.557	3.907	6.814	12.99	26.62	57.35
6.0		1.726	2.039	3.092	5.402	10.40	21.53		1.924	2.689	4.467	8.262	16.53	35.22		2.635	4.024	7.038	13.46	27.59	59.87
0	3	2.222	3.556	5.926	10.16	17.78	31.60	4	3.556	5.926	10.16	17.78	31.60	56.89	5	5.926	10.16	17.78	31.60	56.89	103.4
.06		2.222	3.556	5.929	10.17	17.82	31.73		3.556	5.926	10.16	17.80	31.68	57.10		5.926	10.16	17.79	31.64	57.02	103.8
.12		2.224	3.557	5.939	10.21	17.95	32.07		3.558	5.930	10.18	17.87	31.89	57.71		5.929	10.16	17.81	31.76	57.39	104.9
.24		2.233	3.573	5.988	10.37	18.41	33.32		3.573	5.954	10.26	18.14	32.69	59.90		5.954	10.21	17.95	32.22	58.80	108.8
.36		2.258	3.613	6.088	10.64	19.12	35.16		3.613	6.022	10.43	18.59	33.93	63.14		6.022	10.32	18.24	33.02	60.48	114.6
.48		2.307	3.692	6.254	11.03	20.08	37.49		3.692	6.154	10.71	19.26	35.59	67.25		6.153	10.55	18.73	34.20	63.92	121.9
.545		2.347	3.756	6.379	11.31	20.71	38.97		3.756	6.260	10.92	19.74	36.69	69.56		6.260	10.73	19.10	35.03	65.87	126.6
.6		2.386	3.820	6.502	11.56	21.29	40.31		3.819	6.366	11.13	20.18	37.70	72.23		6.366	10.91	19.46	35.81	67.67	130.8
.8		2.543	4.072	6.982	12.57	23.53	45.47		4.071	6.787	11.95	21.92	41.63	81.36		6.786	11.63	20.88	38.88	74.65	147.2
1.0		2.696	4.319	7.455	13.57	25.78	50.72		4.317	7.199	12.75	23.65	45.55	90.62		7.198	12.34	22.28	41.91	81.63	163.8
1.5		3.030	4.861	8.508	15.84	31.00	63.24		4.855	8.100	14.54	27.56	54.67	112.7		8.097	13.89	25.39	48.80	97.89	203.4
2.0		3.294	5.294	9.366	17.74	35.49	74.36		5.283	8.822	15.99	30.83	62.51	132.3		8.814	15.12	27.92	54.53	111.7	238.3
2.4		3.465	5.574	9.927	19.09	38.51	81.98		5.559	9.288	16.95	32.99	67.76	145.7		9.277	15.92	29.67	58.33	121.0	262.3
3.0		3.663	5.901	10.59	20.48	42.10	91.03		5.881	9.833	18.06	35.54	73.99	161.7		9.816	16.85	31.51	62.80	132.0	290.8
4.0		3.873	6.216	11.27	21.97	45.62	99.91		6.221	10.41	19.22	38.11	80.13	177.2		10.39	17.84	33.51	67.31	142.9	318.5
6.0		3.990	6.435	11.63	22.76	47.45	104.3		6.408	10.72	19.84	39.47	83.31	184.9		10.70	18.38	34.60	69.71	148.6	332.3